PII S0016-7037(01)00580-4

High-resolution strontium isotope stratigraphy across the Cambrian-Ordovician transition

S. EBNETH,[1] G. A. SHIELDS,[2,*] J. VEIZER,[2,3] J. F. MILLER,[4] and J. H. SHERGOLD[5]

[1]Formerly Institut für Geologie, Mineralogie und Geophysik, Ruhr Universität, 44780 Bochum, Germany
[2]Ottawa-Carleton Geoscience Centre, University of Ottawa, Ontario K1N 6N5, Canada
[3]Institut für Geologie, Mineralogie und Geophysik, Ruhr Universität, 44780 Bochum, Germany
[4]Geography, Geology and Planning Department, Southwest Missouri State University, Springfield, Missouri 65804-0089, USA
[5]La Freunie, Benayes, 19510 Masseret, France

Abstract—We have analyzed 214 fossil apatite samples from nine stratigraphic sections worldwide that cover the lower Cambrian to lower Ordovician for their strontium isotope ratios. Of these samples, 180 from six sections that cover the Cambrian-Ordovician transition (<5 Ma) reveal how the extent of isotopic alteration can differ greatly according to lithology and sample type. From three limestone sections, 126 euconodont samples yield the most consistent $^{87}Sr/^{86}Sr$ ratios and are used in this article to constrain seawater $^{87}Sr/^{86}Sr$ across the Cambrian-Ordovician boundary. By contrast, protoconodonts, paraconodonts, and inarticulate brachiopods are far less likely to retain a primary $^{87}Sr/^{86}Sr$ signature and appear to be of only limited value for chemostratigraphy. Seawater $^{87}Sr/^{86}Sr$ fell from maximum values for the Phanerozoic of more than 0.7092 during the early Late Cambrian to 0.7090 by the earliest Ordovician. High-resolution sampling has permitted the recognition of sinusoidal variations with a wavelength on the order of <1 Ma that are superimposed on the overall fall in $^{87}Sr/^{86}Sr$. These variations may be caused by high-order cycles in seawater $^{87}Sr/^{86}Sr$ or diagenetic alteration. *Copyright © 2001 Elsevier Science Ltd*

1. INTRODUCTION

Marine authigenic minerals, if unaltered, retain the strontium isotopic composition of the seawater in which they precipitated. By analyzing stratigraphically well-constrained marine carbonates, phosphates, and barites for their $^{87}Sr/^{86}Sr$ ratios, we can reconstruct temporal variations in seawater Sr isotopic composition. Such $^{87}Sr/^{86}Sr$ curves can be used for global chemostratigraphic correlation as well as global tectonic interpretation (Veizer, 1989), provided that the oceans have always been isotopically homogeneous with respect to strontium, which appears likely due to the long residence time of Sr in seawater (Holland, 1984). The roots of modern Sr isotope stratigraphy can be found with Peterman et al. (1970), who were the first to demonstrate unequivocally that seawater $^{87}Sr/^{86}Sr$ did not increase unidirectionally with time (Wickman, 1948) but has instead varied around a mean value of 0.7080 since the Cambrian. Veizer and Compston (1974) supplied additional constraints on these fluctuations before a concerted effort by researchers at Mobil led to the construction of the first Phanerozoic $^{87}Sr/^{86}Sr$ curve (Burke et al., 1982). This curve, although comprehensive for most of the Phanerozoic, did not cover the entire Cambrian period, and related publications provide no biostratigraphic information for the lower Paleozoic parts of the curve (e.g., Denison et al., 1998). Subsequent studies, only some of which incorporate biostratigraphy (Keto and Jacobsen, 1987; Donnelly et al., 1988, 1990; Gao and Land, 1991; Montañez et al., 1996, 2000; Saltzman et al., 1995), have constrained seawater $^{87}Sr/^{86}Sr$ to ≥0.7090 during the Middle and Late Cambrian. As part of a much wider chemostratigraphic study covering the entire pre-Cenozoic

Phanerozoic (Veizer et al., 1999), the present contribution seeks to constrain seawater $^{87}Sr/^{86}Sr$ during the Cambrian-Ordovician transition using well-preserved fossil apatite. In addition, this study aims to assess the suitability for Sr isotope stratigraphy of various groups of skeletal phosphate (euconodonts, paraconodonts, protoconodonts, and inarticulate brachiopods). To achieve adequate coverage, samples from nine carefully selected sections from around the world were analyzed (Fig. 1). Six of these sections cover the Cambrian-Ordovician boundary interval only (Fig. 2).

2. DEFINITION AND AGE OF THE CAMBRIAN-ORDOVICIAN BOUNDARY

Fossiliferous sedimentary rocks of this age are widespread, and global stratigraphic correlation is made easier by the combination of three fossil groups of high stratigraphic potential, the trilobites, graptolites, and conodonts, the latter two being particularly cosmopolitan in nature. This allowed Norford (1988) to write on behalf of the working group on the Cambrian-Ordovician boundary that "sequences can be correlated with one another with considerable precision." As a result of a plenary session of this working group in 1985, it was decided that the boundary be placed at a horizon just below the first influx of nematophorous (planktic) graptolites and should be selected on the basis of conodont biozones. After much detailed work, nematophorous graptolites are now believed to appear almost everywhere in the world within the *Iapetognathus* conodont Zone (Ross et al., 1997; Cooper, 1999; Nicoll et al., 1999). The present status of the Cambrian-Ordovician boundary is that a GSSP (global stratotype section and point) has been accepted at Green Point, Newfoundland, at the incoming of *Iapetognathus fluctivagus*. This decision, as well as the suggestion that the Tremadoc be the initial stage of the Ordovician system, has been approved by the Subcommission on

---

*Author to whom correspondence should be addressed (gshields@ science.uottawa.ca).
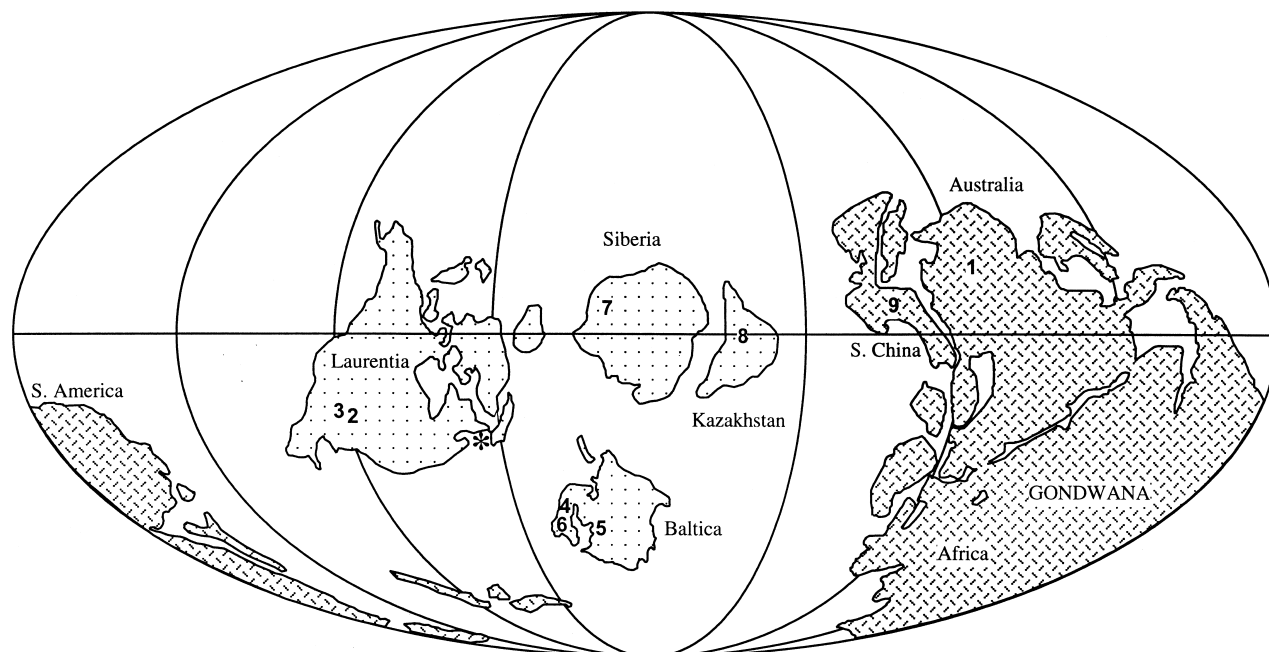
Fig. 1. Paleogeographic reconstruction for the earliest Ordovician after Scotese and McKerrow (1991) with section locations marked 1 to 9 as in text. Cambrian-Ordovician boundary sections are shown bold. *indicates the location of the newly ratified basal Ordovician GSSP in Newfoundland, Canada.

Ordovician Stratigraphy and the Board of the Commission on Stratigraphy and has been ratified by the International Union of Geological Sciences (IUGS). The actual datum is just above the base of the *Cordylodus lindstromi* conodont Zone at Green Point (Nicoll et al., 1999). The Green Point boundary stratotype in Newfoundland appears to present problems for detailed chemostratigraphy because strata at this section contain sediment and fossils that were possibly eroded and redeposited from shallower facies (James and Stevens, 1986; Barnes, 1988; Miller and Flokstra, 1999). In this report, we present data from sections that show no indication of sedimentary redeposition and mixing with the exception of the *Obolus*-Sandstone of Estonia. We present biostratigraphic data from each section, but we make no attempt to correlate these sections directly with the newly defined stratotype section for the base of the Ordovician system.

Until recently, there were no precise geochronologic ages between 526 Ma for the mid-Lower Cambrian of South Australia (Cooper et al., 1992) and 473 Ma for the upper Arenig, Lower Ordovician of Newfoundland (Dunning and Krogh, 1991). This led to considerable uncertainty regarding the age of the Cambrian-Ordovician boundary as well as the duration of Late Cambrian biozones, the only constraint being a Rb/Sr isochron age of 501 ± 7 Ma from uppermost Cambrian shales in China (Chen et al., 1988). In addition, certain SHRIMP U/Pb ages, such as the 526 Ma above, have been questioned on the basis of biostratigraphic ambiguity and analytical uncertainty (Jago and Haines, 1998). The commonly cited age of 510 Ma for the Cambrian-Ordovician boundary (Harland et al., 1990) now appears to be too old. Davidek et al. (1998) report a U/Pb zircon age of 491 ± 1 Ma for a volcaniclastic sandstone within the lower *Peltura scarabaeoides* Zone at Ogof-ddû, near Cric-

cieth, North Wales, which is situated 16 m beneath the lowest occurrence of the lower Tremadocian dendroid *Rhabdinopora flabelliformis socialis*. The dated level lies demonstrably within the uppermost Cambrian, and the authors correlate the dated sandstone to a position below *Cordylodus proavus* Zone sediments elsewhere. A revision of the Cambrian-Ordovician boundary to ~490 Ma can be envisaged. Such a young age is further confirmed by a U/Pb zircon age from an uppermost Tremadocian K-bentonite from Cape Breton island of 483 ± 1 Ma (Landing et al., 1997) and by a young age of ~509 Ma for the uppermost Lower Cambrian of New Brunswick (Landing et al., 1998). We consider that the Middle-Late Cambrian boundary lies at ~499 Ma (e.g., Perkins and Walshe, 1993) while noting that some workers prefer an older age closer to 505 Ma (Jago and Haines, 1998). All the above ages, which are used in this article (Fig. 2) are consistent with the recommendations of Young and Laurie (1995).

3. SAMPLE MATERIAL

Previous studies have demonstrated that low-Mg calcite is the most likely of the common marine precipitates to preserve the $^{87}Sr/^{86}Sr$ ratio of seawater over geologic time scales (Veizer et al., 1999). Low-Mg calcite fossil tests, if well preserved, can be used to reconstruct variations in seawater $^{87}Sr/^{86}Sr$, with foraminifera (Cretaceous until Recent), belemnites (Mesozoic), and articulate brachiopods (Ordovician until Recent) having been widely used for this purpose in recent years. However, although low-Mg calcite skeletal fauna first appear in the geologic record in the Lower Cambrian, they are commonly too rare and delicate to be used for this purpose in the Cambrian System, with the possible exception of trilobite components

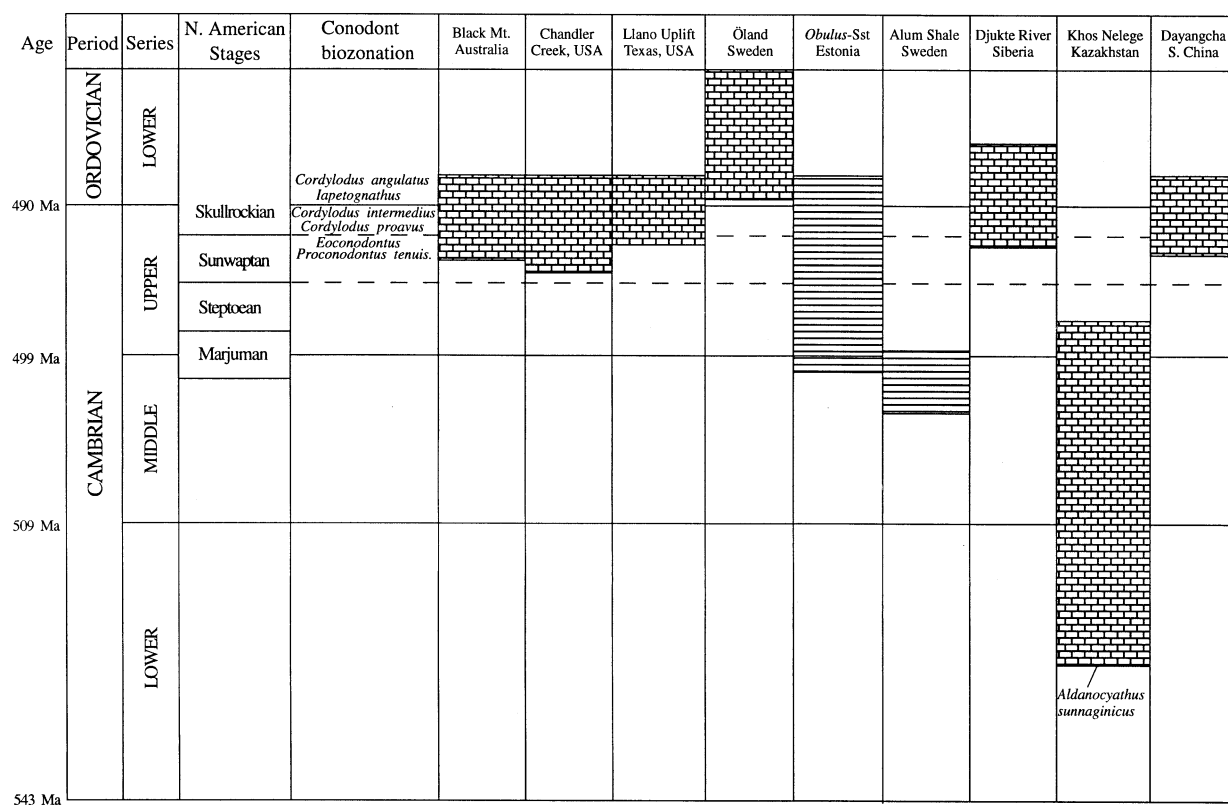| Age	Period	Series	N. American Stages	Conodont biozonation	Black Mt. Australia	Chandler Creek, USA	Llano Uplift Texas, USA	Öland Sweden	*Obulus*-Sst Estonia	Alum Shale Sweden	Djukte River Siberia	Khos Nelege Kazakhstan	Dayangcha S. China
490 Ma	ORDOVICIAN	LOWER		*Cordylodus angulatus Iapetognathus*									
	CAMBRIAN	UPPER	Skullrockian	*Cordylodus intermedius Cordylodus proavus Eoconodontus Proconodontus tenuis.*									
			Sunwaptan										
499 Ma			Steptoean										
		MIDDLE	Marjuman										
509 Ma		LOWER										*Aldanocyathus sunnaginicus*	
543 Ma													

Fig. 2. Stratigraphic ranges of studied sections shown as horizontal bricks (limestone dominated) or horizontal planks (silicate dominated). North American stage names are those recommended by Palmer (1998). Age constraints are justified in text.

(Montañez et al., 1996). As a result, this study concentrates on conodont and inarticulate brachiopod apatite, which is sufficiently abundant and permits precise biostratigraphic correlation. Previous work on conodonts has met with varying degrees of success (Bertram et al., 1992; Martin and McDougall, 1995; Ruppel et al., 1996; Ebneth et al., 1997; Qing et al., 1998; Korte, 1999), indicating that conodont $^{87}Sr/^{86}Sr$ may be altered during diagenesis, with the extent of alteration commonly linked to postdepositional heating. During heating, fossil apatite tends to darken, which has permitted a scale of alteration to be established called the conodont Color Alteration Index or CAI (Epstein et al., 1977). Nevertheless, considerable data scatter can still occur in conodont sample sets with low CAIs of 1.0 to 2.5 (e.g., Qing et al., 1998). This is because low-temperature, early diagenetic isotopic exchange may also affect $^{87}Sr/^{86}Sr$, with the extent of deviation from seawater $^{87}Sr/^{86}Sr$ dependent on the amount of exchange and the nature of the surrounding rock matrix. Ebneth et al. (1997) estimated that in their study of Devonian conodonts up to 40% of a conodont's strontium has equilibrated with the matrix. As a result, pure limestone, itself showing little departure from seawater isotopic composition, represents the most desirable matrix. Conversely, conodonts embedded within a clay- or detritus-rich matrix would tend to suffer greater alteration due to the availability of radiogenic Sr. This is especially important in view of the inhomogeneity of trace element concentrations and $^{87}Sr/^{86}Sr$ within the conodont test (Holmden et al., 1996; Korte, 1999). Recent studies indicate that this inhomogeneity may be more extreme in lower Paleozoic conodonts and follows established diagenetic exchange patterns of Mn, and Fe enrichment as well as Sr loss, although diagenetic Sr enrichment may also occur at the rims (Korte, 1999). Other approaches in pre-Ordovician Sr isotope stratigraphy include analyzing rock components such as bulk carbonate (Burke et al., 1982) and early cements or micrite (e.g., Montanez et al., 1996). These methods generally result in considerable data scatter but when combined with trace element work can be of great value in chemostratigraphy in the absence of any fossil tests (Brasier et al., 1996).

4. GEOLOGIC SETTING AND SAMPLE SELECTION

The samples for this study were selected from diverse depositional settings, mostly shallow marine carbonate shelves. Paleogeographic reconstructions (Fig. 1) place these sedimentary basins at equatorial to mid latitudes on five different paleocontinents. On the basis of conodont CAI, which we required to be lower than 2 and which was generally lower than 1.5, nine sections were selected for Sr isotope analysis. These were (1) The Black Mountain (Unbunmaroo) section (Fig. 3) of the eastern Georgina Basin, Australia (Radke, 1981). For this Cambrian-Ordovician section, trilobite (Shergold, 1982) and conodont biostratigraphic studies (Druce and Jones, 1971; Nicoll and Shergold, 1991) as well as magnetostratigraphic and carbon isotope data, (Ripperdan and Kirschvink, 1992; Ripperdan et al., 1993) have been published. Only two formations of interest are present, the upper part of the Chatsworth Lime-
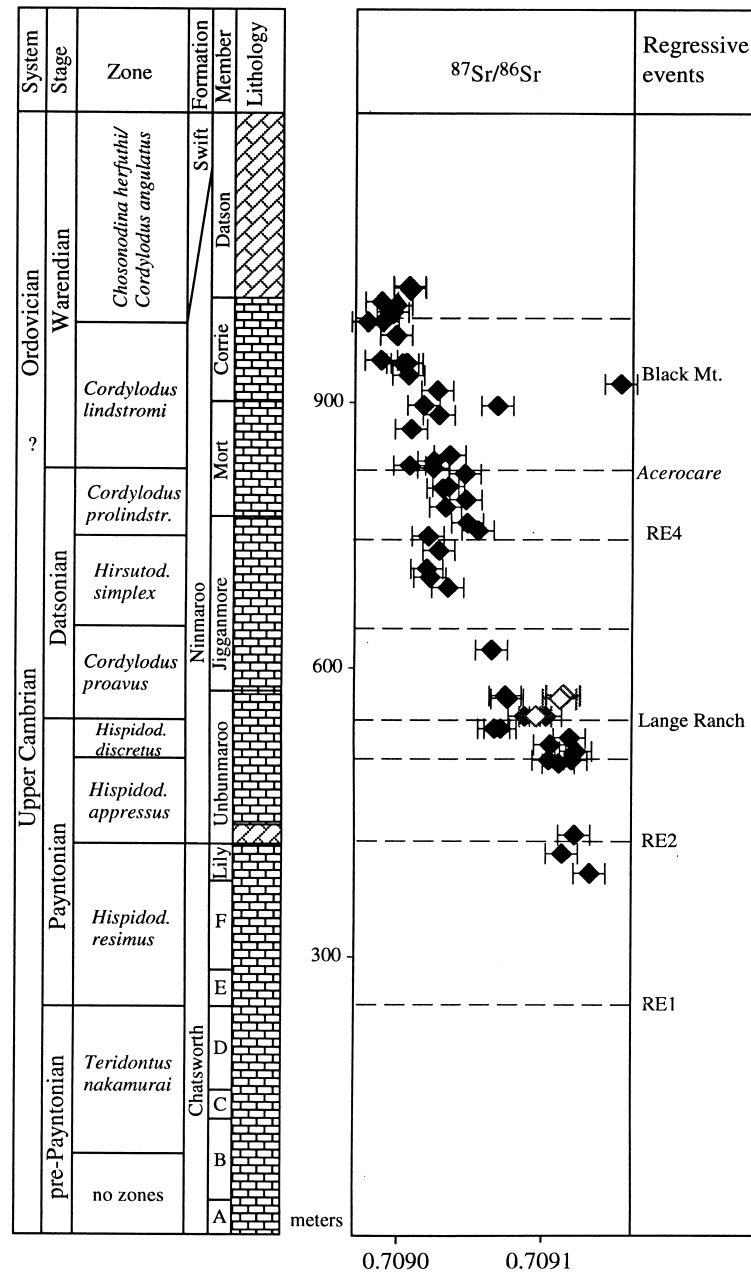
Fig. 3. Sr-isotope stratigraphy of euconodonts from the Black Mountain section, Queensland, Australia. Regressive events are as in Nicoll et al. (1992). Vertical error bars correspond to the generally worst-case 2 standard error analytical precision of $\pm 10 \times 10^{-6}$. Lithology is shown by horizontal bricks (limestone) and slanted bricks (dolostone). Open symbols correspond to calcite matrix.

stone, which consists of a series of upward-shoaling carbonate sequences, and the Ninmaroo Formation, a thick, carbonate-rich unit that covers much of the southeastern Georgina Basin (Druce et al., 1982). Sixty-three analyses were carried out on 49 conodont samples and three samples of matrix from the Black Mountain section. (2) The Chandler Creek section (Fig. 4), Wichita Mountains, Oklahoma, USA, has sometimes been used as a Laurentian reference section for the Cambrian-Ordovician boundary (Stitt et al., 1981). Its conodont biostratigraphy has been studied (Miller et al., 1982), whereas the Arbuckle Group as a whole has been the subject of a whole-rock-based C- and

Sr-isotope study (Gao and Land, 1991). Thirty-three analyses were carried out on 32 conodont samples from the Chandler Creek section. (3) Llano Uplift (Fig. 5): Our high-resolution sampling focussed on the Cambrian-Ordovician Wilberns Formation at Lange Ranch, Welge Ranch and Threadgill Creek (Fig. 5), central Texas, USA. Biostratigraphy of the Llano Uplift is described in Barnes and Bell (1977), Stitt et al. (1981), and Miller (1988)) and carbon isotope stratigraphy in Ripperdan and Miller (1995). Thirty-three analyses were carried out on 29 conodont samples from the Llano Uplift sections. (4) On the island of Öland in Sweden, there is a hiatus close to the
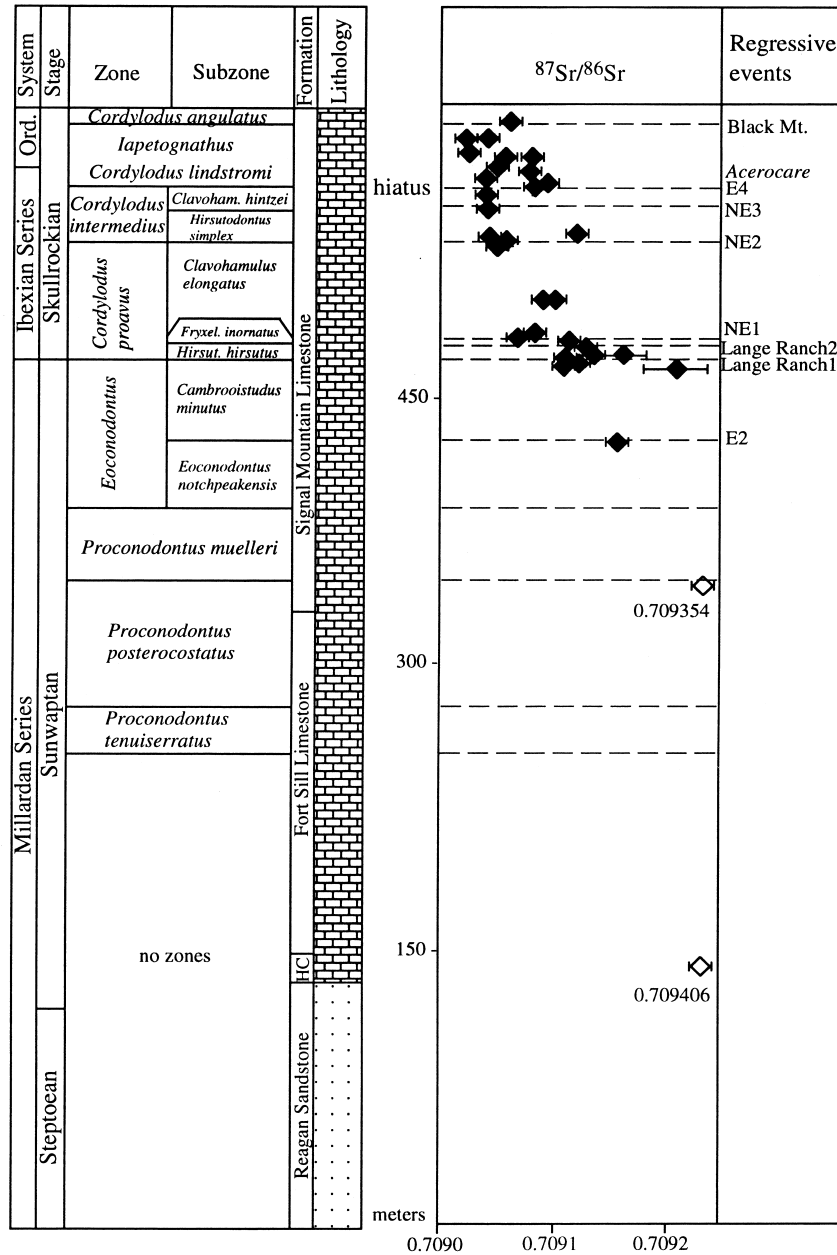
Fig. 4. Sr-isotope stratigraphy of of euconodonts from the Chandler Creek section, Oklahoma, USA. Regressive events are as in Nicoll et al. (1992). Vertical error bars correspond to the generally worst-case 2 standard error analytical precision of $\pm 10 \times 10^{-6}$ (two samples have lower precision). Open symbols correspond to two paraconodont samples.

Cambrian-Ordovician boundary, which appears to diminish in importance toward the south, where it is marked only by a horizon of reworking. Conodonts were sampled from the Lower Ordovician Djupvik and Köpingsklint Formations of Öland, the biostratigraphy of which has been described by van Wamel (1974)). Seven analyses were carried out on four conodont samples from Öland. (5) *Obolus*-Sandstone, Estonia. The Estonian samples consist of exceptionally well-preserved phosphatic inarticulate brachiopods ranging in age from latest Middle Cambrian to earliest Ordovician. Several samples have been reworked from lower formations resulting in considerable uncertainty in biozonation. Eighteen analyses were carried out on 16 brachiopod samples from Estonia. (6) Alum Shale: Paraconodonts from the Upper Cambrian Alum Shale of Sweden were observed early on to be highly altered (See Table 1; Appendix) despite their probable low-temperature history (CAIs cannot be measured for paraconodonts), which led to the abandoning of this part of the study. Nine analyses were carried out on seven paraconodont samples from the Alum Shale. (7) The Djukte River section of the Siberian Platform (Obut, 1989) represents a shallow marine carbonate platform that crosses the Cambrian-Ordovician boundary. G. Abaimova has established a conodont biostratigraphy for this section (pers. comm., 1994). Fourteen analyses were carried out on 14 conodont samples
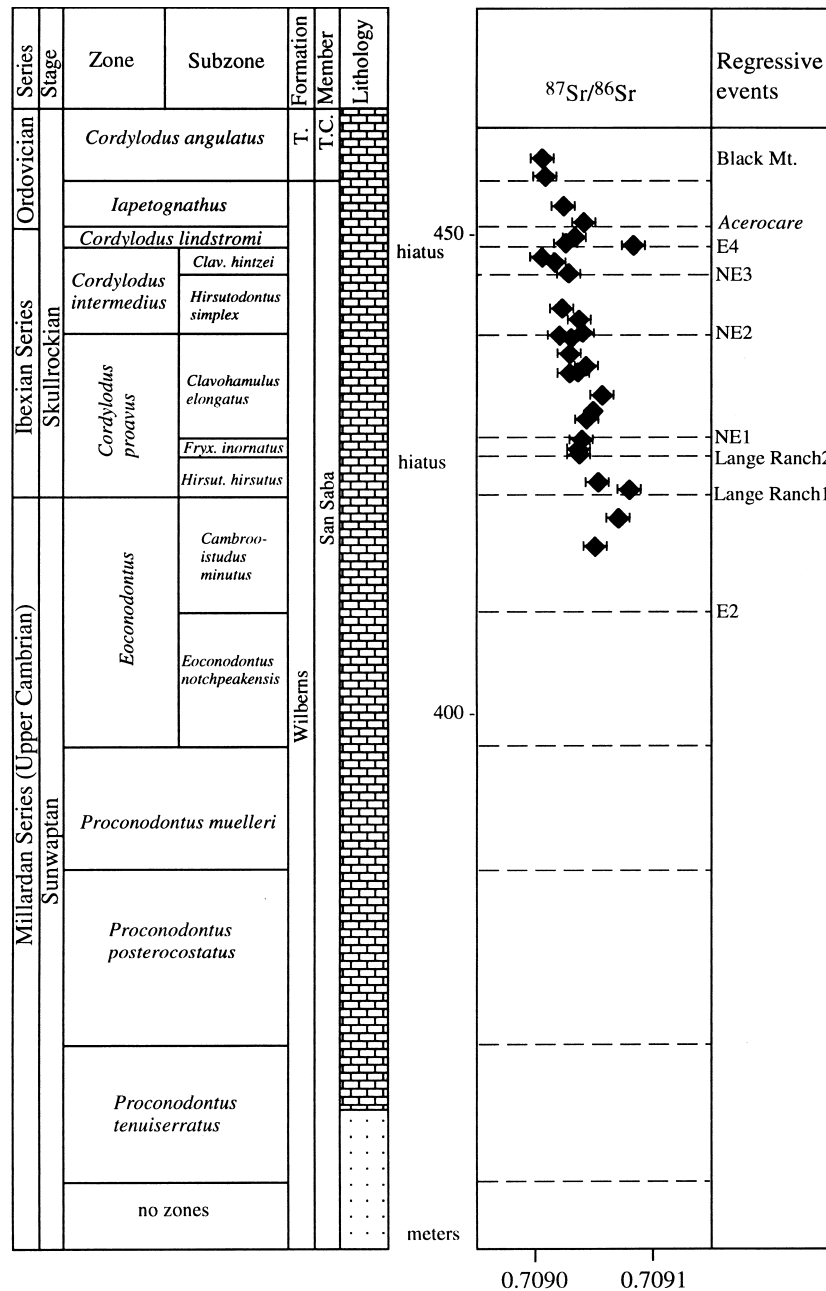
Fig. 5. Sr-isotope stratigraphy of of euconodonts from the Llano Uplift sections, Texas, USA. Regressive events are as in Nicoll et al. (1992). Vertical error bars correspond to the generally worst-case 2 s.e. analytical precision of $\pm 10 \times 10^{-6}$.

from the Djukte section. (8) The Khos-Nelege section (Fig. 6), Karaulakh Mountains of the NE Siberian Platform ranges from the *Aldanocyathus sunnaginicus* Zone of the Lower Cambrian (Tommotian) to the *Parabolinites levis* Zone of the Upper Cambrian. Lithologies are diverse but limestone dominates. Eighteen analyses were carried out on 18 samples of inarticulate brachiopods from the Khos-Nelege section. (9) The Xiao-yangqiao Critical Section, near Dayangcha (Fig. 7), Jilin Province, China, (Chen, 1986; Chen et al., 1988) consists of rythmic alternations of limy mudstones and shales of the Upper Cambrian. Carbon isotope and magnetostratigraphic studies are

reported in Ripperdan et al. (1993). Thirty-seven analyses were carried out on 20 euconodont, 9 paraconodont, 3 protoconodont, and 5 inarticulate brachiopod samples from the Dayangcha section.

5. ANALYTICAL TECHNIQUES

Bulk samples from which fossils were later separated were washed thoroughly, with weathered crusts removed where present. Areas with clearly identifiable fractures or veining were generally not considered for analysis. Further crushing of the samples was followed by dissolution in 5% acetic acid. Every 2 to 3 days, the sample was decanted, the fraction 80 μm to 2 mm being retained, rinsed, and dried at 50°C.
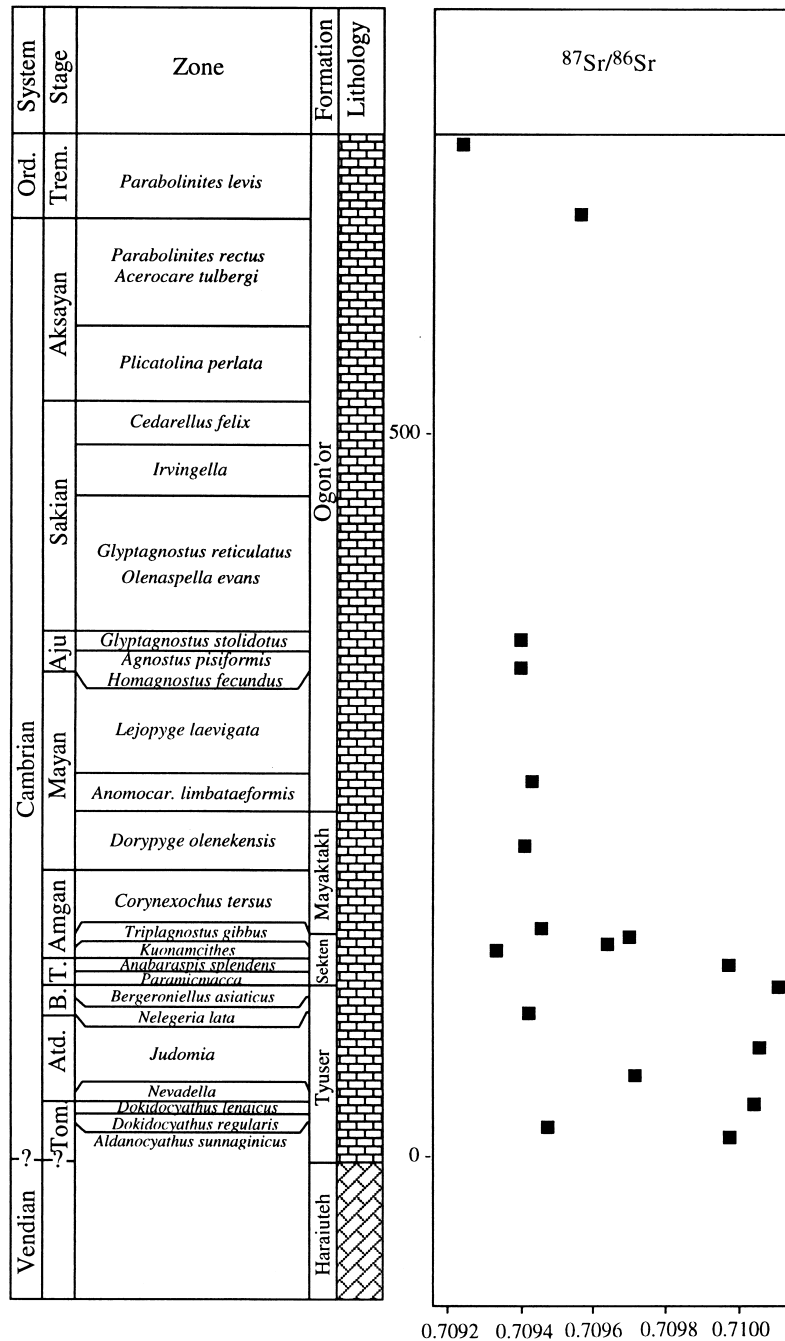
Fig. 6. Sr-isotope stratigraphy of inarticulate brachiopods from the Khos Nelege section, NE Siberia, Russia. Lithology is shown by horizontal bricks (limestone) and slanted bricks (dolostone). Analytical error is contained within symbol.

Fossils were hand picked under a binocular microscope without any further chemical treatment. For conodonts, one to three large or up to 10 small individuals of one particular species were selected and cleaned in an ultrasonic bath until no extraneous material was visible at 64 × magnification. Other phosphatic fossils were prepared in the same way with comparable quantities of phosphate used in the analyses. Reaction took place in a teflon beaker over less than 2 h with approximately 2 mL of 2.5 N HCl. After evaporation and centrifugation, concentration of the strontium was carried out using standard cation exchange techniques (Bio Rad AG50Wx8) with 2.5 N HCl as the sole eluent. Between 150 and 250 ng of strontium was loaded onto a single rhenium filament with a mixed solution of Ta_2O_5–HNO_3–HF–H_3PO_4 (Birck,

1986). Isotopic analyses were carried out at the Ruhr university in Bochum, Germany, using a Finnigan MAT 262 multicollector mass spectrometer with measurement of the NBS SRM 987 standard every 12th sample on average. Sample and literature data have been normalized to our long-term standard value of 0.710231. This mean value represents the average over 4.5 years and 550 measurements and bears a standard deviation (1 SD) of 38×10^{-6} and a standard error of 17×10^{-7}. Further details of standard normalization are given in Diener et al. (1996). A total of 130 measurements of the modern seawater standard USGS Eqn. 1, which is a *Tridachna* from Enewetak Lagoon, Marshall Island, yielded a mean value of $0.709145 \pm 32 \times 10^{-6}$ (1 SD) over the same period.
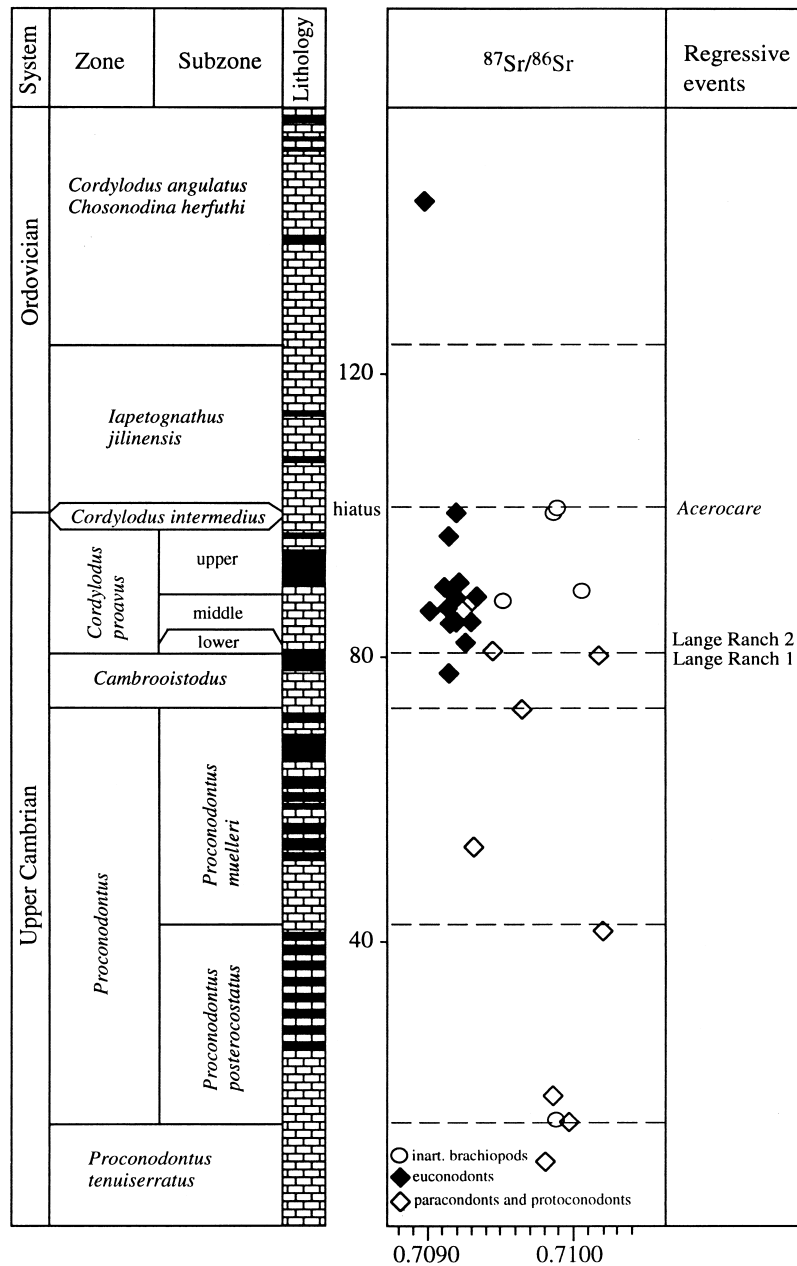
Fig. 7. Sr-isotope stratigraphy of various phosphatic fossil-types from the Dayangcha section, Jilin, China. Regressive events are as in Nicoll et al. (1992). Lithology is shown by horizontal bricks (limestone) and dark areas (siliciclastics). Analytical error is contained within symbol.

6. RESULTS

Black Mountain, western Queensland, Australia: $^{87}Sr/^{86}Sr$ decreases from 0.709120 ± 0.000010 in the *Hispidodontus resimus* and *Hispidodontus appressus* Zones of the Upper Cambrian to 0.708990 ± 0.000010 by the *Cordylodus angulatus* Zone of the Lower Ordovician (Fig. 3). High-resolution features with amplitudes $\leq 50 \times 10^{-6}$ are discernible, especially close to the Payntonian-Datsonian Stage boundary and across the *Hirsutodontus simplex-Cordylodus prolindstromi* Zone boundary, which also marks a regression (RE 4). Lowest $^{87}Sr/^{86}Sr$ is found within the *Cordylodus lindstomi* Zone (basal

Ordovician). Samples of matrix from the *Cordylodus proavus* Zone yielded similar or only slightly more radiogenic $^{87}Sr/^{86}Sr$ ratios (up to 40×10^{-6}) than selected *Teridontus* conodonts from the same rock sample, which indicates that the $^{87}Sr/^{86}Sr$ ratios of the conodonts are well preserved. Comparison between samples from the same stratigraphic level shows that variation can reach 50×10^{-6} (e.g., sample GB90 to 002/89).

Chandler Creek, Wichita Mtns., Oklahoma: $^{87}Sr/^{86}Sr$ generally decreases, reaching an initial maximum nick point at the base of the *Cordylodus proavus* Zone (Fig. 4). At the boundary between the *Fryxellodontus inornatus* and the *Clavohamulus*

elongatus Subzones, there is an abrupt drop of 50×10^{-6} to 0.709064, whereafter ^{87}Sr/^{86}Sr decreases further. As with the Black Mountain section, ^{87}Sr/^{86}Sr attains minimum values (0.709040 ± 0.000020) within the *Cordylodus lindstromi* Zone (above the first appearance of the Lower Ordovician marker fossil *Iapetognathus*). Two paraconodont samples from the base of the section yielded significantly more radiogenic ratios of around 0.7093 to 4.

Llano Uplift, Texas: ^{87}Sr/^{86}Sr decreases from a high of 0.709081 at the base of the *Cordylodus proavus* Zone to a low around 0.709000 at the base of the Lower Ordovician *Corylodus angulatus* Zone (Fig. 5). In contrast with the above two sections, there are no significant kicks in ^{87}Sr/^{86}Sr at conodont zone boundaries and recognized levels of hiatus. The one exception to this is an increase of 76×10^{-6} from the *Cordylodus intermedius* to the *Cordylodus lindstromi* Zone, although this increase is not sustained. This level represents a significant hiatus in both this section and the Chandler Creek section and corresponds to the *Cordylodus prolindstromi* Zone in the Black Mountain section, Australia.

Baltica: ^{87}Sr/^{86}Sr (not plotted in any figure) from the Lower Ordovician of Öland (Appendix) decreases from 0.709060 in the *Drepanodus deltifer* Zone to an average of 0.708902 in the *Paroistodus evae* Zone, which is consistent with euconodont-based data in Qing et al. (1998). By contrast, Cambrian paraconodont samples from the Alum Shale of Sweden yielded highly radiogenic ^{87}Sr/^{86}Sr of between 0.7103 and 0.7162 that point to pervasive postdepositional alteration, which has rendered these paraconodonts useless for chemostratigraphy. Inarticulate brachiopods from the Middle Cambrian–Lower Ordovician of Estonia show a bipolar ^{87}Sr/^{86}Sr distribution with a range of 300×10^{-6}. The bipolar nature of these data (see Appendix) serves to mask any primary, stratigraphic variation that might have been present and may be the result of redeposition. ^{87}Sr/^{86}Sr ratios of apparently in situ samples from the Ülgase and Maardu Formations record little change in ^{87}Sr/^{86}Sr, from 0.709102 to 0.709139.

Siberia: ^{87}Sr/^{86}Sr (not plotted in any figure) decreases from 0.709029 in the Upper Cambrian *Eoconodontus* Zone to 0.708922 in the Tremadocian "Fauna C" Zone (Appendix). At the base of the next faunal zone, zone D, which corresponds to a new formation (Ugorsian Horizon), there is a jump to lower ^{87}Sr/^{86}Sr, 0.70873, although there is considerable dispersion in the data at this level (210×10^{-6}).

Kazakhstan: ^{87}Sr/^{86}Sr for inarticulate brachiopods of the Khos Nelege section of Kazakhstan (Fig. 6) shows considerable dispersion throughout the Cambrian, with highly radiogenic ratios between 0.709218 and 0.710095. Upper and Middle Cambrian forms possess more consistent lowermost ratios from 0.709325 to 0.709385 through 230 m of section. Only these lowermost ^{87}Sr/^{86}Sr ratios are comparable with "least-altered" literature data for this time (Montañez et al., 1996, 2000).

Dayangcha, Jilin Province, China: ^{87}Sr/^{86}Sr dispersion appears to be systematic here (Fig. 7), with inarticulate brachiopod strontium being consistently more radiogenic by up to 800×10^{-6} than euconodonts from the same stratigraphic level. *Prooneotodus rotundatus* (paraconodont) and *Phakelodos tenuis* (protoconodont) samples are also anomalously radiogenic, averaging 0.7098 compared with 0.7092 for euconodonts. Although some paraconodonts yielded credible ^{87}Sr/

^{86}Sr, euconodont ^{87}Sr/^{86}Sr is more consistent. The *Cordylodus proavus* Zone at Dayangcha section was sampled intensively. The lower part of this zone yielded euconodont ^{87}Sr/^{86}Sr of 0.709175 and 0.709290, the middle part between 0.709051 and 0.709330, and the upper part between 0.709152 and 0.709382. The lowest value derives from the basal Ordovician *Cordylodus angulatus* Zone: 0.709026.

7. DISCUSSION

Apatite fossils are often used only reluctantly to reconstruct seawater ^{87}Sr/^{86}Sr because of a general inconsistency of results compared with low Mg-calcite fossils, such as articulate brachiopods. For example, Ebneth et al. (1997) demonstrated that conodont ^{87}Sr/^{86}Sr was systematically more radiogenic, by up to 0.0001, than coeval brachiopods from the same section (Diener et al., 1996). On the other hand, some studies report little deviation between the two fossil-types (e.g., Qing et al., 1998), whereas Korte (1999) has demonstrated that among equally well-preserved fossils from the Triassic, conodonts actually experienced less isotopic exchange than brachiopods from the same section. Theoretical modeling (Ebneth et al., 1997) has shown that the susceptibility of conodonts to low-temperature diagenetic alteration is due to isotopic exchange with the surrounding matrix, which can lead to an isotopic shift of at least one third of the difference between the two end members. Therefore, given the appropriate matrix type (i.e., marine limestone rather than detrital silicate), phosphatic fossils may record primary variations in seawater ^{87}Sr/^{86}Sr to the same level of resolution as calcitic brachiopods. Applying this rationale to our study would help to explain why the Alum Shale phosphatic brachiopods are so radiogenic (Fig. 8). Isotopic exchange is also likely to explain why there is so much dispersion in data from the Dayangcha section (Figs. 7 and 8), which comprises alternating limestone and detrital units. Only lowermost ^{87}Sr/^{86}Sr ratios from both Dayangcha and Khos-Nelege show expected seawater values (Denison et al., 1998; Montañez et al., 2000), indicating that there has been addition of ^{87}Sr from detrital silicate during diagenesis. The systematic nature of ^{87}Sr/^{86}Sr variation at Dayangcha reveals that euconodonts are more likely than protoconodonts, paraconodonts, and inarticulate brachiopods to preserve seawater ^{87}Sr/^{86}Sr.

Isotopic alteration is also possible in a limestone-dominated system, making analysis of the rock matrix desirable, as was possible for the Black Mountain section (Appendix). For the Llano Uplift sections, euconodont ^{87}Sr/^{86}Sr is perfectly consistent with previously published low-Mg calcite cement data (Johnson and Goldstein, 1993), suggesting that minimal isotopic exchange has taken place here as well. In both these sections, data dispersion for any particular stratigraphic level is limited to 100×10^{-6} for any given biozone (Figs. 3 and 5) and is generally better than 50×10^{-6}. This level of agreement compares favorably with calcitic brachiopod ^{87}Sr/^{86}Sr, which commonly shows up to 50×10^{-6} variability even locally for the same stratigraphic level (e.g., Diener et al., 1996; Azmy et al., 1999).

7.1. Cambrian-Ordovician Transition ^{87}Sr/^{86}Sr

As argued above, sample sets that show significantly greater scatter, markedly radiogenic ratios, or both are likely to be

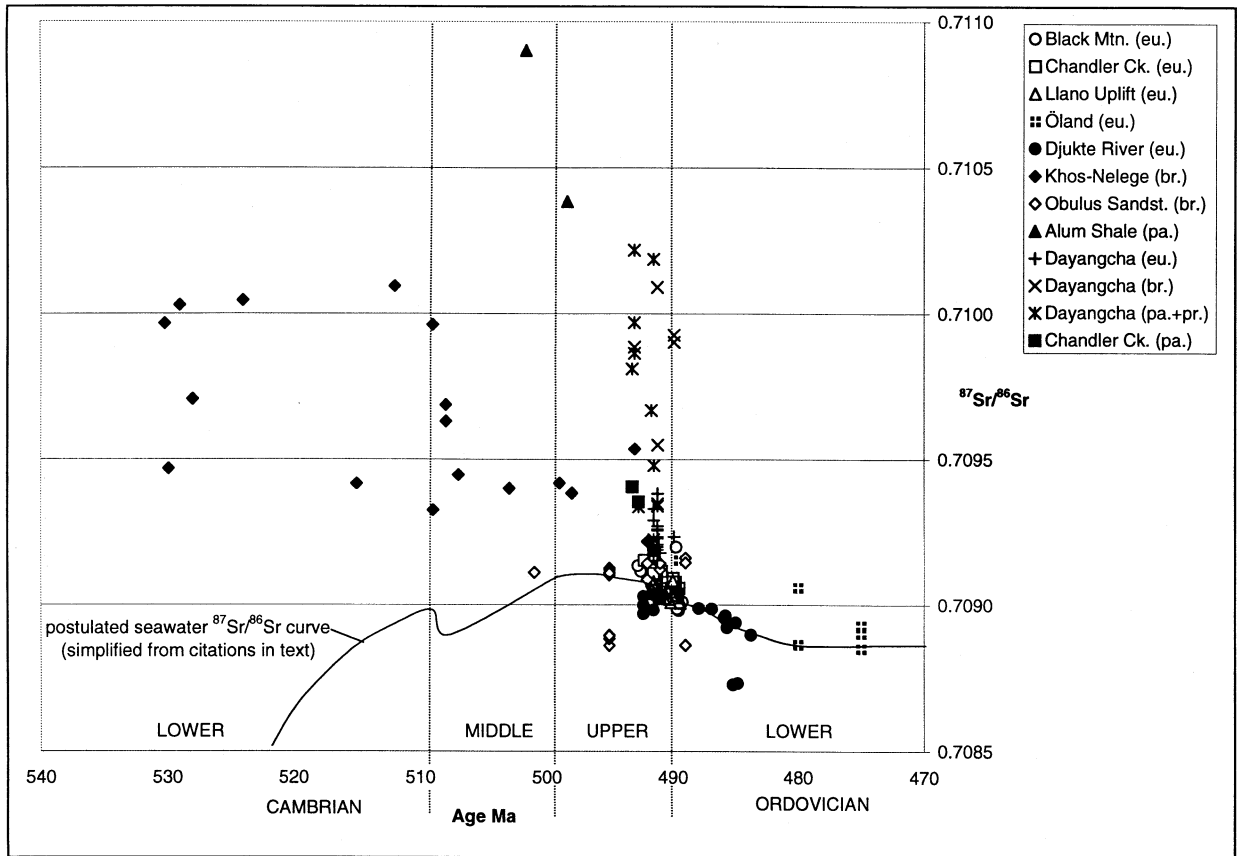Fig. 8. 87Sr/^{86}Sr for all nine sections investigated. Only the two lowest ^{87}Sr/^{86}Sr ratios are shown for the Alum Shale.
eu. = euconodonts; pa. = paraconodonts; pr. = protocondonts; br. = inarticulate brachiopods.

altered. This is certainly the case for the Alum Shale (our section 6), lower Khos Nelege (section 8), and most Dayangcha (section 9) data. By contrast, ^{87}Sr/^{86}Sr ratios from inarticulate brachiopods of the *Obulus* Sandstone of Estonia (section 5) appear to be anomalously low (Fig. 8). As the true biostratigraphic affinities of most of these Estonian samples is unsure, it is impossible at present to ascertain whether these low ^{87}Sr/^{86}Sr ratios (see Appendix) represent altered marine values, redeposition, or both. The above four sections therefore are excluded from further discussion of seawater ^{87}Sr/^{86}Sr across the Cambrian-Ordovician transition. Of the five sections that remain, neither the Öland (section 4) nor the Djukte (section 7) sections cover the Cambrian-Ordovician transition interval at sufficient resolution to permit detailed interregional comparison. Therefore, our discussion of seawater ^{87}Sr/^{86}Sr across the Cambrian-Ordovician transition will focus mainly on the euconodont-bearing limestone sections of Black Mountain (no. 1), Chandler Creek (no. 2), and Llano Uplift (no. 3).

^{87}Sr/^{86}Sr data for 126 conodonts from these three sections reveal that seawater ^{87}Sr/^{86}Sr decreased from 0.70912 to 0.70900 from the beginning of the late Late Cambrian (*Eoconodontus* Zone, Australia) to the earliest Ordovician (Fig. 9). All three sections show distinct higher order features with amplitudes $\leq 50 \times 10^{-6}$ that have been superimposed on the first order fall in ^{87}Sr/^{86}Sr. Several of these features are related to sedimentary condensation and hiatus at Black Mountain and

Chandler Creek, which would tend to support a primary origin. Similar features have been reported from elsewhere in the Paleozoic using both euconodonts (Cummins and Elderfield, 1994; Diener et al., 1996; Ruppel et al., 1996) and calcitic brachiopods (Ebneth et al., 1997). However, the amplitudes of many of these features are within the current de facto limit of resolution of Sr isotope stratigraphy, sometimes called the geologic reproducibility, of no better than about $\pm 30 \times 10^{-6}$ (Diener et al., 1996; Veizer et al., 1999).

Such high-order variations, if primary, would imply relatively rapid <1 Ma changes in global seawater ^{87}Sr/^{86}Sr that seem incompatible with the long residence time of Sr in seawater today (Ruppel, 1996). To accommodate this problem, Cummins and Elderfield (1994) considered that such cyclicity must reflect sinusoidal variations in the Sr, and possibly riverine, flux, combined with a shorter ocean residence time for Sr of about one third that of today, that is, 0.8 Ma. Although this is feasible, a considerably shorter Sr ocean residence time might also lead to resolvable isotopic inhomogeneity in seawater. This would be unfortunate because ^{87}Sr/^{86}Sr homogeneity is one of the essential assumptions in Sr isotope stratigraphy.

It is also possible that high-order ^{87}Sr/^{86}Sr variations arise through the radioactive decay of ^{87}Rb or through diagenetic alteration, both of which may be related to subtle lithologic changes. Although Rb was not measured during our study, published Rb concentrations in conodonts and other forms of
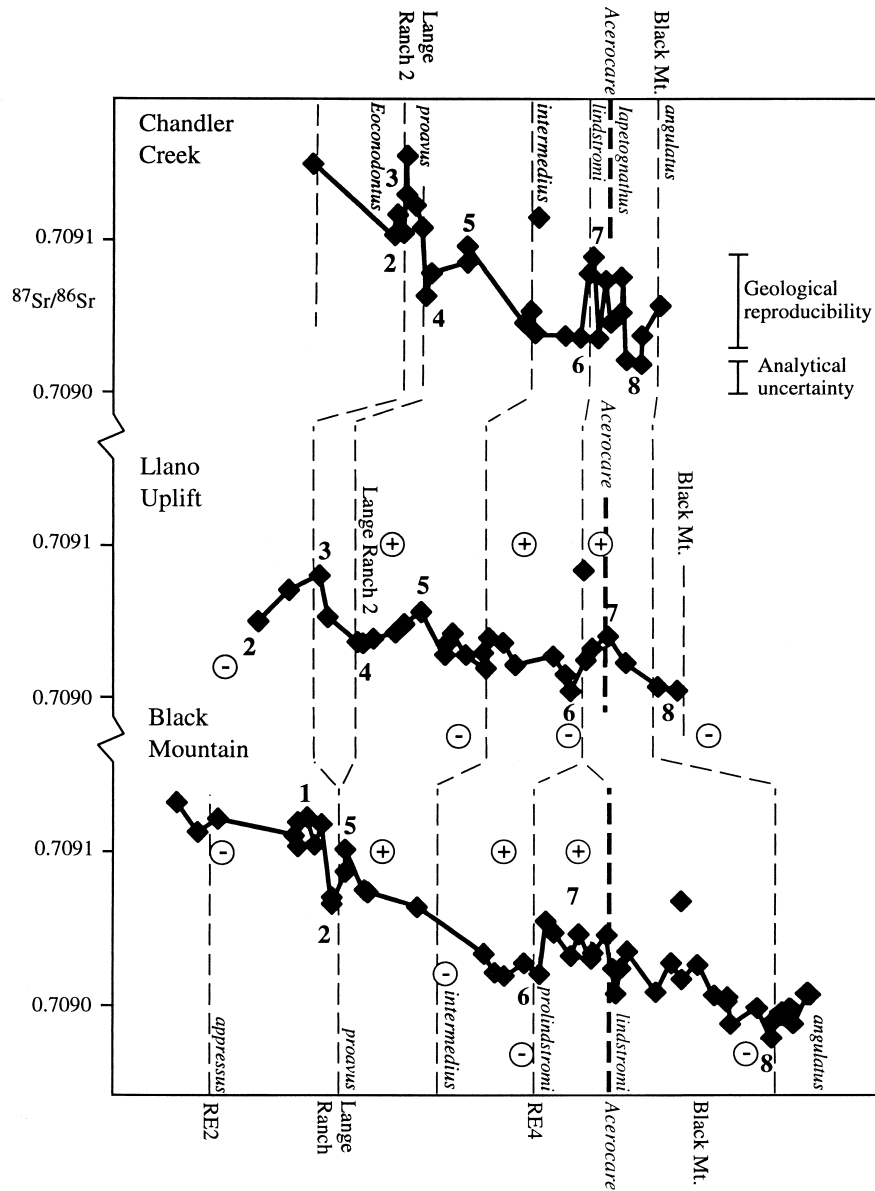
Fig. 9. 87Sr/^{86}Sr trends across the Cambrian-Ordovician transition at the Black Mountain, Chandler Creek, and Llano Uplift limestone-dominated sections. Vertical broken lines show conodont zones with probable Cambrian-Ordovician boundary shown in bold. Correlation of major regressive events Lange Ranch, Acerocare, and Black Mountain is also attempted (after Nicoll et al., 1992). δ^{13}C maxima (+) and minima (−) are from Black Mountain (Ripperdan et al., 1992) and Lawson Cove, Utah (Ripperdan and Miller, 1995). Areas numbered 1 to 8 are Sr isotope excursions identified in this study.

skeletal apatite are consistently low enough to have negligible effect on measured ^{87}Sr/^{86}Sr. For example, a Rb concentration of 1 ppm, which is a realistic maximum value for conodonts (Ebneth et al., 1997), would result in a difference of only 11 × 10^{-6} in the measured ^{87}Sr/^{86}Sr of a typical 500 Ma old conodont with 2000 ppm Sr. The possible effects of diagenetic alteration are more difficult to determine and have been shown to lead occasionally to apparent cyclicity in ^{87}Sr/^{86}Sr (e.g., Reinhardt et al., 2000). In the study of Ebneth et al. (1997), some high-order features were found in both brachiopod and conodont ^{87}Sr/^{86}Sr records from the same sections, which led these authors to interpret the variations as primary. However, it

could also be argued that both sets of trends have been influenced by subtle diagenetic isotopic exchange, especially considering the consistently more radiogenic and clearly altered nature of the conodonts (Diener et al., 1996; Ebneth et al., 1997). In another study, Ruppel et al. (1996) reported high-order variations in conodont ^{87}Sr/^{86}Sr through the Silurian. However, a later, higher resolution study on pristine brachiopods from the Silurian found no evidence for such high-order variations (Azmy et al., 1999). Similarly, the very low amplitude ^{87}Sr/^{86}Sr features reported by Cummins and Elderfield (1994) from the Carboniferous, have not been reproduced by subsequent studies (Bruckschen et al., 1995). Therefore, al-

though <1 Ma cyclicity in seawater $^{87}Sr/^{86}Sr$ is certainly feasible, we must acknowledge that an equally strong case can be made for a more localized or diagenetic origin, whereas the possibility of shorter residence times for Sr in the oceans could cause paleogeographic variation in seawater $^{87}Sr/^{86}Sr$. To demonstrate the primary and global nature of high-order variations in $^{87}Sr/^{86}Sr$, statistically significant variations need to be identified from paleogeograpically distant sites of identical stratigraphic level, something that requires considerable biostratigraphic precision. Such evidence would make it unlikely that diagenetic alteration, ocean inhomogeneity, or analytical artifacts were the cause.

Figure 9 attempts to correlate the Black Mountain, Chandler Creek and Llano Uplift sections by means of biostratigraphy and regressive events (Nicoll et al., 1992), which allows $^{87}Sr/^{86}Sr$ excursions (numbered 1–8) to be compared. $\delta^{13}C$ excursion maxima and minima are also shown superimposed on the $^{87}Sr/^{86}Sr$ trends using data from Black Mountain (Ripperdan et al., 1992) and Lawson Cove, Utah (Ripperdan and Miller, 1995). These data tend to support the current biostratigraphic correlation between the Australian and the U.S. sections (Ripperdan and Miller, 1995). The *Euconodontus–Cordylodus proavus* Zone boundary is associated with a drop in $^{87}Sr/^{86}Sr$ at all three sections. Erosion at Black Mountain at this level, which corresponds to the Lange Ranch Regression Event (Nicoll et al., 1992), may have removed also some of the detail of the Llano Uplift section, whereas condensation may have had a similar effect at Chandler Creek (Fig. 9). Using current stratigraphic control, however, it is difficult to establish the precise contemporaneity of these isotopic excursions. In all three sections, a second major fall in $^{87}Sr/^{86}Sr$ occurs from the basal *Cordylodus proavus* Zone to the top of the *Cordylodus intermedius* Zone (features 5–6 in Fig. 9). There follows a rise in $^{87}Sr/^{86}Sr$ to the *Cordylodus lindstromi* Zone. According to carbon isotope evidence reported by Ripperdan and Miller (1995) and correlation of the global *Acerocare* regression event by Nicoll et al. (1992), excursion 7 at Llano Uplift (33×10^{-6}) would correlate with the *Hirsutodontus simplex–Cordylodus prolindstromi* Zone boundary at Black Mountain, which exhibits a jump of 37×10^{-6}. At Chandler Creek, sampling resolution and data dispersion make it difficult to identify a similar high-order feature there.

Recognition of comparable trends in all three sections is consistent with a common, possibly global, origin. However, the incompleteness of the geologic record, as witnessed by the hiatuses in all three sections, makes the correlation of these excursions impossible to prove at present. Despite similarities in the $^{87}Sr/^{86}Sr$ records of at least two distant sections, Black Mountain and Llano Uplift, most of the correlatable higher order features possess amplitudes ~30 to 50×10^{-6}, which is close to, or lower than, any plausible geologic limit of uncertainty (cf. Veizer et al., 1999). An additional worry is that despite elimination of obviously altered samples, silicate-hosted fossils, all noneuconodont phosphatic fossils, extreme outliers, and sample sets with poor sampling coverage, absolute $^{87}Sr/^{86}Sr$ ratios are still not always comparable between sections. For example, mean $^{87}Sr/^{86}Sr$ for *Cordylodus proavus* Zone samples range from 0.709103 (Chandler Creek) and 0.709100 (Black Mountain) to 0.709037 (Llano Uplift) and 0.709006 (Djukte), a difference of almost 100×10^{-6}. Al-

though, such differences could be considered the inevitable result of primary within-zone (or paleogeographic) variation in $^{87}Sr/^{86}Sr$, such a large difference between the otherwise similar, neighboring sections of Chandler Creek and Llano Uplift is unlikely to be primary. Indeed, mean $^{87}Sr/^{86}Sr$ at Chandler Creek is consistently more radiogenic than at Llano Uplift for every biozone, which implies that diagenetic alteration has significantly affected the Chandler Creek data. Whatever the cause of such high-order trends in $^{87}Sr/^{86}Sr$, their existence, coupled with the complications of diagenetic alteration in even apparently well-preserved euconodonts, places severe limits on the reproducibility of Sr-isotope-based correlation, which in this case cannot be better than the time equivalent of 60×10^{-6}. Because the rate of change of seawater $^{87}Sr/^{86}Sr$ is very gradual close to the Cambrian-Ordovician transition, this translates to no better than ±5 to 10 Ma.

7.2. Comparison with Literature Data and Geologic Interpretation

These results fit into a growing $^{87}Sr/^{86}Sr$ database. Gao and Land (1991) reported bulk-rock $^{87}Sr/^{86}Sr$ data from the Upper Cambrian and Lower Ordovician. Importantly, they demonstrated that dolomitization had caused $^{87}Sr/^{86}Sr$ to decrease in some of their samples, whereas diagenetic alteration of some limestones had caused $^{87}Sr/^{86}Sr$ to increase. The combination of these two effects led to considerable scatter in their data of greater than 200×10^{-6}. Nevertheless, their data reveal a rough trend toward lower $^{87}Sr/^{86}Sr$ ratios through the Cambrian-Ordovician transition, which is broadly consistent with our results. Johnson and Goldstein (1993) determined more precisely the Sr isotopic composition of Cambrian-Ordovician seawater by analyzing bladed low-Mg calcite cements in hardgrounds from the Wilberns Formation, Texas, yielding 0.70905 to 6, which is identical to conodont-based data from the same formation herein (Llano Uplift; Fig. 5). Saltzman et al. (1995) reported micrite data from the *Elvinia* (uppermost Steptoean) and *Taenicephalus* Biozones (basal Sunwaptan Stage) of the Wind River Range, Wyoming, that reveal a significant fall in $^{87}Sr/^{86}Sr$ from ~0.70920 to 0.70907. Our data from the Sunwaptan stage at Chandler Creek (Fig. 4) are considerably more radiogenic than these results, which confirms that the Chandler Creek paraconodonts are altered. Montañez et al. (1996) reported data for the upper Middle and basal Upper Cambrian platform carbonates of the southern Great Basin. These authors selected well-preserved carbonate components such as micrite, marine cements, and trilobite parts, using various petrographic criteria and trace element characteristics to constrain seawater $^{87}Sr/^{86}Sr$ to ≤0.70918 and ≤0.70922 within the *Crepicephalus* and *Cedaria* Zones of the lowermost Upper Cambrian (Marjuman), respectively.

Previous studies indicate, therefore, that seawater $^{87}Sr/^{86}Sr$ attained exceptionally high values of at least 0.7092 during the early-to-mid Late Cambrian (end-Marjuman to end-Steptoean), which is before the deposition of the euconodonts analyzed in this study. Seawater $^{87}Sr/^{86}Sr$ may have been even higher, up to 0.7093 (our data from Khos Nelege, Fig. 6; Montañez et al., 2000). The significance of this maximum can be assessed by translating $^{87}Sr/^{86}Sr$ ratios into εSr values, which correspond to

the deviation of seawater $^{87}Sr/^{86}Sr$ from contemporary mantle $^{87}Sr/^{86}Sr$.

$$\varepsilon Sr = [(^{87}Sr/^{86}Sr_{seawater}/^{87}Sr/^{86}Sr_{mantle\ input}) - 1] * 10000$$

To calculate εSr, it is necessary to estimate the evolution of the $^{87}Sr/^{86}Sr$ of mantle input. To do this, we need to assume a certain geochemical homogeneity among mantle sources, which allows us to remove the effect of the decay of radioactive ^{87}Rb to ^{87}Sr through time. Published estimates indicate that mantle Rb/Sr is close to 0.027, and its $^{87}Sr/^{86}Sr$ ratio is ~0.704 (Faure, 1986).

Recalculation of seawater $^{87}Sr/^{86}Sr$ to εSr has the desirable effect of pinning down one of the two main sources of strontium in seawater, marine volcanic exchange, and therefore provides us with a more reliable way of comparing the relative importance of continental weathering versus mantle input through time. To illustrate this, εSr today is $+ 73.4$ ($^{87}Sr/^{86}Sr = 0.70916$), whereas the εSr decrease from the late Cambrian high to the Early Ordovician is likely to have been from about $+ 83.0$ to $+ 78.6$ ($^{87}Sr/^{86}Sr = 0.7093-0.7090$). Such high εSr for the Cambrian-Ordovician transition implies that late Cambrian seawater chemistry was considerably more dominated by continental weathering input than it is today. This may be explained as the effect of unroofing highly radiogenic, metamorphic rocks in the Damara Belt as part of the Pan-African orogeny (Montañez et al., 2000), which could be analogous to the process operating today in the Himalayan region (e.g., Richter et al., 1992). Seawater $^{87}Sr/^{86}Sr$ began to rise toward this maximum by the Early Cambrian Tommotian and Atdbanian Stages (e.g., Brasier et al., 1996), which are only poorly constrained in time to between 534 Ma and 520 Ma (Landing et al., 1998). This places the rate of increase in seawater $^{87}Sr/^{86}Sr$ at between $30 \times 10^{-6}\ Ma^{-1}$ and 60×10^{-6} Ma^{-1} during much of the Cambrian, which is comparable with $40 \times 10^{-6}\ Ma^{-1}$ during the Cenozoic.

9. CONCLUSIONS

Our study shows that limestone-hosted euconodonts with low CAI (<2) can be used to pinpoint seawater $^{87}Sr/^{86}Sr$ during the early Paleozoic. Such material is generally better for this purpose than carbonate rock components and compares favorably with well-preserved calcitic brachiopods. Other types of fossil apatite, such as protoconodonts, paraconodonts, and inarticulate brachiopods, are less likely to retain primary Sr isotope signatures even when otherwise apparently unaltered. Seawater $^{87}Sr/^{86}Sr$ attained Phanerozoic maximum levels of at least 0.70920 during the early Late Cambrian, whereafter $^{87}Sr/^{86}Sr$ dropped progressively reaching 0.70900 by the earliest Ordovician. Low-amplitude, high-order sinusoidal variations in $^{87}Sr/^{86}Sr$ with a wavelength of <1 Ma may be related to primary variation in seawater $^{87}Sr/^{86}Sr$ or diagenetic alteration. Interregional correlation of some of these high-order features implies a primary origin. However, some of these features and especially the often significant differences in absolute $^{87}Sr/^{86}Sr$ between neighboring sections can be put down to diagenetic alteration. Several factors conspire to constrain the best possible resolution of global strontium isotopic correlation around the Cambrian-Ordovician transition to no better than $\pm 30 \times 10^{-6}$, which corresponds to ± 5 to 10 Ma.

REFERENCES

Azmy K., Veizer J., Wenzel B., Bassett M. G., and Copper P. (1999) Silurian strontium isotope stratigraphy. *Geol. Soc. Am. Bull.* **111,** 475–483.

Barnes C. R. (1988) The proposed Cambrian-Ordovician global boundary stratotype and point (GSSP) in western Newfoundland, Canada. *Geol. Mag.* **125,** 381–414.

Barnes V. E., and Bell W. C. (1977) *The Moore Hollow Group of Central Texas.* University of Texas at Austin, Bureau of Economic Geology, Report of investigations **88,** 169 p.

Bertram C. J., Elderfield H., Aldridge R. J., and Conway-Morris S. (1992) $^{87}Sr/^{86}Sr.$, $^{143}Nd/^{144}Nd$ and REEs in Silurian phosphatic fossils. *Earth Planet. Sci. Lett.* **113,** 239–249.

Birck J. L. (1986) Precision K-Rb-Sr isotopic analysis: Application to Rb-Sr chronology. *Chem. Geol.* **56,** 73–83.

Brasier M. D., Shields G., Kuleshov V. N., and Zhegallo Le, A. (1996) Integrated chemo- and biostratigraphic calibration of early animal evolution of southwest Mongolia. *Geol. Mag.* **133,** 445–485.

Bruckschen P., Bruhn F., Veizer V., and Buhl D. (1995) $^{87}Sr/^{86}Sr$ isotope evolution of Lower Carboniferous seawater: Dinantian of western Europe. *Sediment. Geol.* **100,** 63–81.

Burke W. H., Denison R. E., Hetherington E. A., Koepnik R. B., Nelson H. F., and Otto J.B. (1982) Variations of seawater $^{87}Sr/^{86}Sr$ through Phanerozoic time. *Geology* **10,** 516–519.

Chen J.-Y. (ed.) (1986) *Aspects of the Cambrian-Ordovician boundary in Dayangcha, China.* China Prospect Publishing House, Beijing.

Chen J.-Y., Qian Y.-Y., Zhang J.-M., Lin Y.-K., Yin l.-M., Wang Y.-X., Wang Z.-Z., Yang J.-D., and Wang Y.-X. (1988) The recommended Cambrian-Ordovician global boundary stratotype of the Xiaoyangqiao section (Dayangcha, Jilin Province, China). *Geol. Mag.* **125,** 415–444.

Cooper J. A., Jenkins R. J. F., Compston W., and Williams I. S. (1992) Ion-probe zircon dating of a mid-Early Cambrian tuff in South Australia. *J. Geol. Soc. (London)* **149,** 185–192.

Cooper R. A. (1999) The Ordovician time scale calibration of graptolite and conodont zones. *Acta Universitatis Carolinae* **43,** 1–5.

Cummins D. I. and Elderfield H. (1994) The strontium isotopic composition of Brigantian (late Dinantian) seawater. *Chem. Geol.* **118,** 255–270.

Davidek K., Landing E., Bowring S. A., Westrop S. R., Rushton W. A., Fortey R. A., and Adrain J. M. (1998) New uppermost Cambrian U-Pb date from Avalonian Wales and age of the Cambrian-Ordovician boundary. *Geol. Mag.* **135,** 305–309.

Denison R. E., Koepnik R. B., Burke W. H., and Hetherington E. A. (1998) Construction of the Cambrian and Ordovician seawater $^{87}Sr/^{86}Sr$ curve. *Chem. Geol.* **152,** 325–340.

Diener A., Ebneth S., Veizer J., and Buhl D. (1996) Strontium isotope stratigraphy of the Middle Devonian: Brachiopods and conodonts. *Geochim. Cosmochim. Acta* **60,** 639–652.

Donnelly T. H., Shergold J. H., and Southgate P. N. (1988) Anomalous geochemical signals from phosphatic Middle Cambrian rocks in the southern Georgia Basin, Australia. *Sedimentology* **35,** 549–570.

Donnelly T. H., Shergold J. H., Southgate P. N., and Barnes C. J.

(1990) Events leading to global phosphogenesis around the Protero-
zoic/Cambrian boundary. In *Phosphorite research and development*
(eds. A. J. G. Notholt and I. Jarvis). Geol. Soc. (London) Spec. Publ.
52, 273–287.

Druce E. C. and Jones P. J. (1971) Cambrian-Ordovician conodonts
from the Burke River structural belt, Queensland. *BMR Bull. Austral.
Geol. Geophys.* **110,** 1–159.

Druce E. C., Shergold J. H., and Radke B. M. (1982) A reassessment
of the Cambrian-Ordovician boundary section at Black Mountain,
western Queensland, Australia. In *The Cambrian-Ordovician
Boundary: Sections, Fossil Distributions, and Correlations* (eds.
M. G. Bassett and W. T. Dean). National Museum of Wales, Geol.
Series 3, Cardiff., pp. 193–209.

Dunning G. R. and Krogh T. E. (1991) Stratigraphic correlation of the
Appalachian Ordovician using advanced U-Pb zircon geochronology
techniques. *Geol. Surv. Canada Paper*, 90-9: 85–92.

Ebneth S., Diener A., Buhl D., and Veizer J. (1997) Strontium isotope
systematics of conodonts: Middle Devonian, Eifel Mountains, Ger-
many. *Palaeogeog., Palaeoclim., Palaeoecol.* **132,** 79–96.

Epstein A. G., Epstein J. B., and Harris L. D. (1977) Conodont color
alteration—an index to organic metamorphism. *USGS Professional
Paper* **995,** 1–27.

Faure G. (1986) *Principles of isotope geology*. Wiley, New York.

Gao G. and Land L. S. (1991) Geochemistry of Cambrian-Ordovician
Arbuckle Limestone, Oklahoma: Implications for diagenetic ^{18}O
alteration and secular ^{13}C and $^{87}Sr/^{86}Sr$ variation. *Geochim. Cosmo-
chim. Acta* **55,** 2911–2920.

Harland W. B., Armstrong R. L., Cox A. V., Craig L. E., Smith A. G.
and Smith D. G. (1990) *A Geological Timescale 1989.* Cambridge
University Press, Cambridge, UK.

Holland H. D. (1984) *The Chemical Evolution of the Atmosphere and
the Oceans.* Princeton University Press.

Holmden C., Creaser R. A., Muehlenbachs K., Bergstrom S. M., and
Leslie S. A. (1996) Isotopic and elemental systematics of Sr and Nd
in 454 Ma biogenic apatites: Implications for paleoseawater studies.
Earth Planet. Sci. Lett. **142,** 425–437.

Jago J. B. and Haines P. W. (1998) Recent radiometric dating of some
Cambrian rocks in southern Australia: relevance to the Cambrian
time scale. *Revista Espanola de Paleontologia,* 115–122.

James N. P. and Stevens R. K. (1986) Stratigraphy and correlation of
the Cambro-Ordovician Cow Head Group, western Newfoundland.
Geol. Surv. Canada Bull. 366, 143 pp.

Johnson W. J. and Goldstein R. H. (1993) Cambrian seawater pre-
served as inclusions in marine low-magnesium calcite cement. *Na-
ture* **362,** 335–337.

Keto L. S. and Jacobsen S. B. (1987) Nd and Sr isotopic variation of
Early Paleozoic oceans. *Earth Planet. Sci. Lett.* **84,** 27–41.

Korte C. (1999) $^{87}Sr/^{86}Sr$, $\delta^{18}O$ und $\delta^{13}C$-Evolution des triassischen
Meerwassers: Geochemische und stratigraphische Untersuchungen
an Conodonten und Brachiopoden. *Bochumer geologische und
geotechnische Arbeiten* 52, 171 pp.

Landing E., Bowring S. A., Fortey R. A., and Davidek K. L. (1997)
U-Pb zircon date from Avalonian Cape Breton Island and geochro-
nologic calibration of the Early Ordovician. *Canadian J. Earth Sci.*
34, 724–730.

Landing E., Bowring S. A., Davidek K. L., Westrop S. R., Geyer G.,
and Heldmaier W. (1998) Duration of the Early Cambrian: U-Pb
ages of volcanic ashes from Avalon and Gondwana. *Canadian J.
Earth Sci.* **35,** 329–338.

Martin E. E. and McDougall J. D. (1995) Sr and Nd isotopes at the
Permian/Triassic boundary: a record of climate change. *Chem. Geol.*
125, 73–99.

Miller J. F. (1988) Conodonts as stratigraphic tools for redefinition and
correlation of the Cambrian-Ordovician Boundary. *Geol. Mag.* **125,**
349–362.

Miller J. F. and Flokstra B. R. (1999) Graphic correlation of important
Cambrian-Ordovician boundary sections. Quo vadis Ordovician.
Short papers of the Eighth International Symposium on the Ordovi-
cian System. *Acta Universitis Carolinae, Geologica* **43,** 81–84.

Miller J. F., Taylor M. E., Stitt J. H., Etherington R. L., Hintze L. F.,
and Taylor J. F. (1982) Potential Cambrian-Ordovician boundary
stratotypes in the western United States. In *The Cambrian-Ordovi-
cian Boundary: Sections, Fossil Distributions, and Correlations.*

(eds. M. G. Bassett and W. T. Dean). National Museum of Wales,
Geol. Series 3, Cardiff, pp. 155–180.

Montañez I. P., Banner J. L., Osleger D. A., Borg L. E., and Bosserman
P. J. (1996) Integrated Sr isotope variations and sea-level history of
Middle to Upper Cambrian platform carbonates: Implications to the
evolution of Cambrian seawater. *Geology* **24,** 917–920.

Montañez I. P., Osleger D. A., Banner J. L., Mack L. E., and Musgrove
M. (2000) Evolution of the Sr and C isotope composition of Cam-
brian oceans. *GSA Today* **10,** 5, 1–10.

Nicoll R. S. and Shergold J. H. (1991) Revised Late Cambrian (pre-
Paytonian-Datsonian) conodont biostratigraphy at black Mountain,
Georgina Basin, western Queensland, Australia. *BMR J. Austral.
Geol. Geophys.* **12,** 93–118.

Nicoll R. S., Laurie J. R., Shergold J. S., and Nielson A. T. (1992)
Preliminary correlation of latest Cambrian to early Ordovician sea
level events in Australia and Scandinavia. In *Global Perspectives of
Ordovician Geology* (eds. B. D. Webby and J. R. Laurie) Rotterdam,
pp. 381–394.

Nicoll R. S., Miller J. F., Nowlan G. S., Repetski J. E., and Ethington
R. L. (1999) *Iapetonudus* (New genus) and *Iapetognathus* Landing,
unusual earliest Ordovician multielement conodont taxa and their
utility for biostratigraphy. *Brigham Young University Geology Stud-
ies* **44,** 27–101.

Norford B. S. (1988) Introduction to papers on the Cambrian-Ordovi-
cian boundary. *Geol. Mag.* **125,** 323–326.

Obut A. M. (ed.) (1989) The Ordovician of the Siberian Platform, fauna
and stratigraphy [in Russian]. *Trudy instituta geologii I geophisiki*
751.

Palmer A. R. (1998) A proposed nomenclature for stages and series for
the Cambrian of Laurentia. *Canadian J. Earth Sci.* **35,** 323–328.

Perkins C. and Walshe J. L. (1993) Geochronology of the Mount Read
Volcanics, Tasmania, Australia. *Econ. Geol.* **88,** 1176–1197.

Peterman Z. E., Hedge C. E., and Tourtelot H. A. (1970) Isotopic
composition of strontium in seawater throughout Phanerozoic time.
Geochim. Cosmochim. Acta **34,** 105–120.

Qing H., Barnes C. R., Buhl D., and Veizer J. (1998) The strontium
isotopic composition of Ordovician and Silurian brachiopods and
conodonts: Relationships to geological events and implications for
coeval seawater. *Geochim. Cosmochim. Acta* **62,** 1721–1733.

Radke B. M. (1981) Lithostratigraphy of the Ninmaroo Formation
(Upper Cambrian–Lower Ordovician), Georgina Basin. *Report BMR
Bull. Austral. Geol. Geophys.* **181,** 1–143.

Reinhardt E. G., Cavazza W., Patterson R. T., and Blenkinsop J. (2000)
Differential diagenesis of sedimentary components and the implca-
tion for strontium isotope analysis of carbonate rocks. *Chem. Geol.*
164, 331–343.

Richter F. M., Rowley D. B., and DePaolo D. J. (1992) Sr isotope
evolution of seawater: The role of tectonics. *Earth Planet. Sci. Lett.*
109, 11–23.

Ripperdan R. L. and Kirschvink J. L. (1992) Paleomagnetic results
from the Cambrian-Ordovician boundary section at Black Mountain,
Georgina Basin, western Queensland, Australia. In *Global Perspec-
tives of Ordovician Geology* (eds. B. D. Webby and J. R. Laurie)
Rotterdam, pp. 93–103.

Ripperdan R. L. and Miller J. F. (1995) Carbon isotope ratios from the
Cambrian-Ordovician boundary section at Lawson Cove, Ibex Area,
Utah. In *Ordovician Odyssey: Short papers for the seventh interna-
tional symposium on the Ordovician System* (eds. J. D. Cooper, M. L.
Droser, and S. C. Finney), Pacific Section for Sedimentary Geology
(SEPM), pp. 129–132.

Ripperdan R. L., Margaritz M., Nicoll R. S., and Shergold J. H. (1992)
Simultaneous changes in carbon isotopes, sea level, and conodont
biozones within the Cambrian-Ordovician boundary interval at
Black Mountain, Australia. *Geology* **20,** 1039–1042.

Ripperdan R. L., Magaritz M., and Kirschvink J. L. (1993) Carbon
isotope and magnetic polarity evidence for non-depositional events
within the Cambrian-Ordovician boundary section near Dayangcha,
Jilin Province, China. *Geol. Mag* **130,** 443–452.

Ross R. J. Jr., Hintze L. F., Ethington R. L., Miller J. F., Taylor M. E.,
and Repetski J. E. (1997) The Ibexian, lowermost series in the North
American Ordovician. U.S. Geol. Surv. Prof. Paper, 1579-A.

Ruppel S. C., James E. W., Barrick J. E., Nowlan G., and Uyeno T. T.
(1996) High-resolution $^{87}Sr/^{86}Sr$ chemostratigraphy of the Silurian:

Implications for event correlation and strontium flux. *Geology* **24,** 831–834.

Saltzman M. R., Davidson J. P., Holden P., Runnegar B., and Lohmann K. C. (1995) Sea-level-driven changes in ocean chemistry at an upper Cambrian extinction horizon. *Geology* **23,** 893–896.

Scotese C. R. and McKerrow W. S. (1991) Ordovician plate tectonic reconstructions. In *Advances in Ordovician Geology*. (eds. C. R. Barnes and S. H. Williams) Geol. Surv. Canada Paper 90-9, pp. 271–282.

Shergold J. H. (1982) Late Cambrian (Idamean) trilobites from western Queensland. *BMR Bull. Austral. Geol. Geophys.* **187,** 69 pp.

Stitt J. H., Barnes V. E., Miller J. F., and Taylor J. F. (1981) Cambrian and lowest Ordovician lithostratigraphy and biostratigraphy of southern Oklahoma and central Texas. In *Guidebook for Field Trip* (ed. M. E. Taylor), Vol. 3, 2nd ed. International Symposium on the Cambrian System.

Van Wamel W. A. (1974) Conodont biostratigraphy of the Upper Cambrian and lower Ordovician of northwestern Öland, southeastern Sweden. *Utrecht Micropaleont. Bull.* **10**.

Veizer J. (1989) Strontium isotopes in seawater through time. *Ann. Rev. Earth Planet. Sci.* **17,** 141–167.

Veizer J. and Compston W. (1974) The ^{87}Sr/^{86}Sr composition of seawater during the Phanerozoic. *Geochim. Cosmochim. Acta* **38,** 1461–1484.

Veizer J., Ala D., Azmy K., Bruckschen P., Buhl D., Bruhn F., Carden G. A. F., Diener A., Ebneth S., Godderis Y., Jasper T., Korte C., Pawellek F., Podlaha O., and Strauss H. (1999) ^{87}Sr/^{86}Sr, δ^{13}C and δ^{18}O evolution of Phanerozoic seawater. *Chem. Geol.* **161,** 59–88.

Wickman F. E. (1948) Isotope ratios: A clue to the age of certain marine sediments. *J. Geol.* **56,** 61–66.

Young G. C. and Laurie J. R. (1995) Numerical calibration of major Phanerozoic boundaries. In *An Australian Phanerozoic timescale* (eds. G. C. Young and J. R. Laurie). Oxford Univ. Press, Oxford, pp. 52–59.

APPENDIX

Table 1. ^{87}Sr/^{16}Sr compositions for phosphatic fossils from nine Cambrian-Ordovician sedimentary successions around the world. Height is in meters. Ages have been assigned based on boundary ages of 490 Ma = Cambrian-Ordovician, 499 Ma = Middle-Upper Cambrian, 509 Ma = Lower-Middle Cambrian, 543 Ma = Neoproterozoic-Cambrian (see text for details) and constant duration of conodont biozones of 0.5 Ma. dyn. = dynamic mode, stat. = static mode.

Sample name	Height	Formation	System	Conodont biozone	Conodont material	Age (Ma)	^{87}Sr/^{86}Sr stat.
GB90-003/7	1018.0	Ninmaroo	L. Ordovician	*Cord. angulatus/Chos. her.*	*Cordylodus* sp.	489.2	0.709010
GB90-003/3	1003.0	Ninmaroo	L. Ordovician	*Cord. angulatus/Chos. her.*	*Cordylodus* sp.	489.5	0.708991
GB90-003/1	1002.0	Ninmaroo	L. Ordovician	*Cord. angulatus/Chos. her.*	*Oneotodus* sp.	489.5	0.709000
GB90-002/109	992.0	Ninmaroo	L. Ordovician	*Cord. angulatus/Chos. her.*	*Oneotodus* sp.	489.5	0.708999
GB90-002/107	983.0	Ninmaroo	L. Ordovician	*Cordylodus lindstromi*	*Oneotodus* sp.	489.5	0.708991
GB90-002/107	983.0	Ninmaroo	L. Ordovician	*Cordylodus lindstromi*	mixed species	489.5	0.708981
GB90-002/105	968.5	Ninmaroo	L. Ordovician	*Cordylodus lindstromi*	mixed species	489.6	0.709001
GB90-002/101	942.0	Ninmaroo	L. Ordovician	*Cordylodus lindstromi*	mixed species	489.7	0.708985
GB90-002/99	939.0	Ninmaroo	L. Ordovician	*Cordylodus lindstromi*	mixed species	489.7	0.709009
GB90-002/99	939.0	Ninmaroo	L. Ordovician	*Cordylodus lindstromi*	*Oneotodus* sp.	489.7	0.709005
GB90-002/97	925.5	Ninmaroo	L. Ordovician	*Cordylodus lindstromi*	mixed species	489.7	0.709010
GB90-002/96	915.8	Ninmaroo	L. Ordovician	*Cordylodus lindstromi*	mixed species	489.7	0.709198
GB90-002/95	909.5	Ninmaroo	L. Ordovician	*Cordylodus lindstromi*	mixed species	489.8	0.709030
GB90-002/89	892.0	Ninmaroo	L. Ordovician	*Cordylodus lindstromi*	*Cordylodus lindstromi*	489.8	0.709071
GB90-002/89	892.0	Ninmaroo	L. Ordovician	*Cordylodus lindstromi*	*Oneotodus* sp.	489.8	0.709020
GB90-002/87	888.0	Ninmaroo	L. Ordovician	*Cordylodus lindstromi*	*Oneotodus* sp.	489.8	0.709019
GB90-002/82	882.0	Ninmaroo	L. Ordovician	*Cordylodus lindstromi*	*Oneotodus* sp.	489.8	0.709031
GB90-002/76	867.0	Ninmaroo	L. Ordovician	*Cordylodus lindstromi*	*Oneotodus* sp.	489.9	0.709011
GB90-002/61	837.0	Ninmaroo	L. Ordovician	*Cordylodus lindstromi*	*Oneotodus* sp.	489.9	0.709038
GB90-002/58	832.0	Ninmaroo	L. Ordovician	*Cordylodus lindstromi*	*Oneotodus* sp.	489.9	0.709027
GB90-002/55	828.0	Ninmaroo	L. Ordovician	*Cordylodus lindstromi*	*Oneotodus* sp.	489.9	0.709010
GB90-002/54	827.0	Ninmaroo	L. Ordovician	*Cordylodus lindstromi*	*Oneotodus* sp.	489.9	0.709026
GB90-002/51	824.0	Ninmaroo	L. Ordovician	*Cordylodus lindstromi*	*Oneotodus* sp.	489.9	0.709026
GB90-002/48	818.0	Ninmaroo	U. Cambrian	*Cordylodus prolindstromi*	*Oneotodus* sp.	490.0	0.709049
GB90-002/38	805.0	Ninmaroo	U. Cambrian	*Cordylodus prolindstromi*	*Oneotodus* sp.	490.1	0.709037
GB90-002/34	803.0	Ninmaroo	U. Cambrian	*Cordylodus prolindstromi*	*Oneotodus* sp.	490.2	0.709033
GB90-002/29	790.0	Ninmaroo	U. Cambrian	*Cordylodus prolindstromi*	*Oneotodus* sp.	490.2	0.709049
GB90-002/25	782.0	Ninmaroo	U. Cambrian	*Cordylodus prolindstromi*	*Oneotodus* sp.	490.3	0.709035
GB90-002/14	766.0	Ninmaroo	U. Cambrian	*Cordylodus prolindstromi*	*Oneotodus* sp.	490.4	0.709050
GB90-002/8	757.0	Ninmaroo	U. Cambrian	*Cordylodus prolindstromi*	*Cordylodus* sp.	490.5	0.709057
GB90-002/3	752.0	Ninmaroo	U. Cambrian	*Cordylodus prolindstromi*	*Oneotodus* sp.	490.5	0.709023
BMA 115	735.0	Ninmaroo	U. Cambrian	*Hirsutodontus simplex*	*Oneotodus* sp.	490.7	0.709030
JHS 294.5	714.5	Ninmaroo	U. Cambrian	*Hirsutodontus simplex*	*Oneotodus* sp.	490.8	0.709020
BMA 110	707.0	Ninmaroo	U. Cambrian	*Hirsutodontus simplex*	*Teridontus* sp.	490.9	O.709025
BMA 110	707.0	Ninmaroo	U. Cambrian	*Hirsutodontus simplex*	*Oneotodus* sp.	490.9	0.709025
JHS 276	696.0	Ninmaroo	U. Cambrian	*Hirsutodontus simplex*	*Teridontus* sp.	491.0	0.709036
BMA 108	695.0	Ninmaroo	U. Cambrian	*Hirsutodontus simplex*	*Teridontus* sp.	491.0	0.709035
BMA 108	695.0	Ninmaroo	U. Cambrian	*Hirsutodontus simplex*	*Oneotodus* sp.	491.0	0.709076$^{dyn.}$
BMA 97	627.0	Ninmaroo	U. Cambrian	*Cordylodus proavus*	*Teridontus* sp.	491.3	0.709066
BMA 97	627.0	Ninmaroo	U. Cambrian	*Cordylodus proavus*	*Teridontus* sp.	491.3	0.709086$^{dyn.}$
BMA 95	610.0	Ninmaroo	U. Cambrian	*Cordylodus proavus*	*Teridontus* sp.	491.3	0.709076$^{dyn.}$
BMA 89	577.5	Ninmaroo	U. Cambrian	*Cordylodus proavus*	*Teridontus* sp.	491.5	0.709079
BMA 89	577.5	Ninmaroo	U. Cambrian	*Cordylodus proavus*	matrix	491.5	0.709121
BMA 88	575.0	Ninmaroo	U. Cambrian	*Cordylodus proavus*	*Teridontus* sp.	491.5	0.709081
BMA 88	575.0	Ninmaroo	U. Cambrian	*Cordylodus proavus*	matrix	491.5	0.709119
GB 90-001/41A	564.0	Ninmaroo	U. Cambrian	*Cordylodus proavus*	*Teridontus* sp.	491.5	0.709092
BMA 86	564.0	Ninmaroo	U. Cambrian	*Cordylodus proavus*	matrix	491.5	0.709099
BMA 86	564.0	Ninmaroo	U. Cambrian	*Cordylodus proavus*	*Teridontus* sp.	491.5	0.709106
GB 90-001/31B	550.0	Ninmaroo	U. Cambrian	*Hispidodontus discretus*	*Teridontus* sp.	491.7	0.709073
GB 90-001/31B	550.0	Ninmaroo	U. Cambrian	*Hispidodontus discretus*	*Teridontus* sp.	491.7	0.709068
BMA 82	529.9	Ninmaroo	U. Cambrian	*Hispidodontus discretus*	*Teridontus* sp.	491.9	0.709121
BMA 81	522.5	Ninmaroo	U. Cambrian	*Hispidodontus discretus*	*Teridontus* sp.	491.9	0.709107
GB 90-001/9B	516.0	Ninmaroo	U. Cambrian	*Hispidodontus discretus*	*Teridontus* sp.	492.0	0.709125
GB 90-001/2	507.0	Ninmaroo	U. Cambrian	*Hispidodontus appressus*	*Teridontus* sp.	492.1	0.709122
GB 90-001/2	507.0	Ninmaroo	U. Cambrian	*Hispidodontus appressus*	*Teridontus* sp.	492.1	0.709106
GB 90-001/1	504.0	Ninmaroo	U. Cambrian	*Hispidodontus appressus*	*Teridontus* sp.	492.1	0.709113
BMA 66	427.6	Ninmaroo	U. Cambrian	*Hispidodontus appressus*	*Teridontus* sp.	492.5	0.709124
BMA 66	427.6	Ninmaroo	U. Cambrian	*Hispidodontus appressus*	*Teridontus* sp.	492.5	0.709119$^{dyn.}$
K 143	406.9	Chatsworth	U. Cambrian	*Hispidodontus resimus*	*Teridontus* sp.	492.5	0.709115
BMA 57	386.7	Chatsworth	U. Cambrian	*Hispidodontus resimus*	*Teridontus* sp.	492.7	0.709134
BMA 57	386.7	Chatsworth	U. Cambrian	*Hispidodontus resimus*	*Teridontus* sp.	492.7	0.709125$^{dyn.}$

(Continued)

Table (Continued)

Chandler Creek, Wichita Mountains, Oklahoma, USA (Cambrian-Ordovician transition)

Sample name	Height	Formation	System	Conodont biozone	Conodont material	Age (Ma)	$^{87}Sr/^{86}Sr$ dyn.
CC 1880	574.5	Signal Mtn. L.	L. Ordovician	*Cordylodus angulatus*	*Cordylodus angulatus*	489.5	0.709057
CC 1850	565.5	Signal Mtn. L.	L. Ordovician	*lapetognathus*	*Cordylodus lindstromi*	489.6	0.709038
CC 1848	564.8	Signal Mtn. L.	L. Ordovician	*lapetognathus*	*Cordylodus lindstromi*	489.6	0.709020
CC 1825	557.9	Signal Mtn. L.	L. Ordovician	*lapetognathus*	*Cordylodus* sp.	489.7	0.709022
CC 1815 (M)	554.8	Signal Mtn. L.	L. Ordovician	*lapetognathus*	*Cordylodus* sp.	489.8	0.709057
CC 1814	554.5	Signal Mtn. L.	L. Ordovician	*lapetognathus*	*Cordylodus lindstromi*	489.8	0.709078
CC 1798 (M)	549.7	Signal Mtn. L.	L. Ordovician	*lapetognathus*	*Teridontus nakamurai*	489.9	0.709046
CC 1790 (M)	547.3	Signal Mtn. L.	U. Cambrian	*Cordylodus lindstromi*	*Cordylodus* sp.	490.0	0.709075
CC 1780 M)	544.2	Signal Mtn. L.	U. Cambrian	*Cordylodus lindstromi*	*Teridontus nakamurai*	490.0	0.709036
CC 1769 (M)	540.9	Signal Mtn. L.	U. Cambrian	*Cordylodus lindstromi*	*Cordylodus* sp.	490.0	0.709091
CC 1762 (M)	539.8	Signal Mtn. L.	U. Cambrian	*Cordylodus lindstromi*	*Cordylodus* sp.	490.0	0.709079
CC 1751 (M)	535.5	Signal Mtn. L.	U. Cambrian	*Clavohamulus hintzei*	*Teridontus nakamurai*	490.5	0.709037
CC 1740	528.8	Signal Mtn. L.	U. Cambrian	*Hirsutodontus simplex*	*Cordylodus* sp.	490.6	0.709037
CC 1696 (M)	515.5	Signal Mtn. L.	U. Cambrian	*Hirsutodontus simplex*	mixed species	490.9	0.709116
CC 1687 (M)	512.7	Signal Mtn. L.	U. Cambrian	*Hirsutodontus simplex*	mixed species	490.9	0.709040
CC 1682 (M)	511.2	Signal Mtn. L.	U. Cambrian	*Hirsutodontus simplex*	mixed species	491.0	0.709056
CC 1677.5 (M)	509.8	Signal Mtn. L.	U. Cambrian	*Hirsutodontus simplex*	*Teridontus nakamurai*	491.0	0.709045
CC 1667	506.7	Signal Mtn. L.	U. Cambrian	*Clavohamulus elongatus*	*Cordylodus* sp.	491.0	0.709045
CC 1585 (M)	481.8	Signal Mtn. L.	U. Cambrian	*Clavohamulus elongatus*	*Teridontus nakamurai*	491.2	0.709086
CC 1585 (M)	481.8	Signal Mtn. L.	U. Cambrian	*Clavohamulus elongatus*	*Cordylodus* sp.	491.2	0.709095
CC 1536 (M)	465.5	Signal Mtn. L.	U. Cambrian	*Clavohamulus elongatus*	*Cordylodus proavus*	491.4	0.709080
CC 1525	462.1	Signal Mtn. L.	U. Cambrian	*Clavohamulus elongatus*	*Cordylodus* sp.	491.4	0.709064
CC 1522 (M)	461.2	Signal Mtn. L.	U. Cambrian	*Fryxellodontus inornatus*	*Cordylodus proavus*	491.4	0.709114
CC 1512	458.2	Signal Mtn. L.	U. Cambrian	*Fryxellodontus inornatus*	*Cordylodus proavus*	491.4	0.709127
CC 1500	454.5	Signal Mtn. L.	U. Cambrian	*Hirsutodontus hirsutus*	*Cordylodus proavus*	491.5	0.709134
CC 1497 (M)	453.6	Signal Mtn. L.	U. Cambrian	*Hirsutodontus hirsutus*	*Eoconod. notchpeakensis*	491.5	0.709160
CC 1493 (M)	452.4	Signal Mtn. L.	U. Cambrian	*Hirsutodontus hirsutus*	*Cordylodus proavus*	491.5	0.709107
CC 1483	449.4	Signal Mtn. L.	U. Cambrian	*Hirsutodontus hirsutus*	*Eoconod. notchpeakensis*	491.5	0.709120
CC 1479 (M)	448.2	Signal Mtn. L.	U. Cambrian	*Cambrooistodus minutus*	*Eoconod. notchpeakensis*	491.5	0.709108
CC 1475	447.0	Signal Mtn. L.	U. Cambrian	*Cambrooistodus minutus*	*Eoconod. notchpeakensis*	491.5	0.709206
CC 1347	408.2	Signal Mtn. L.	U. Cambrian	*Eoconodontus notchpeakensis*	*Eoconod. notchpeakensis*	492.3	0.709153
CC 1110	336.4	Signal Mtn. L.	U. Cambrian	*Proconodontus mulleri*	*Prooneotodus rotundatus*	492.7	0.709354
CC 446	135.2	H.C.	U. Cambrian	no zonation	*Proconod. tenuiserratus*	493.2	0.709406

Lange Ranch, Welge Ranch, and Threadgill Creek, Llano uplift, Texas, USA (Cambrian-Ordovician transition)

Sample name	Height	Formation	System	Conodont biozone	Conodont material	Age (Ma)	$^{87}Sr/^{86}Sr$ dyn.
LR 172	461.5	Tanyard	L. Ordovician	*Cordylodus angulatus*	*Cordylodus lindstromi*	489.4	0.709006
LR 166	459.7	Tanyard	L. Ordovician	*Cordylodus angulatus*	*Cordylodus rotundatus*	489.5	0.709009
LR 154	456.4	Wilberns	L. Ordovician	*lapetognathus*	*Cordylodus lindstromi*	489.7	0.709024
LR 145	453.6	Wilberns	L. Ordovician	*lapetognathus*	*Cordylodus lindstromi*	489.8	0.709041
LR 139	451.7	Wilberns	U. Cambrian	*Cordylodus lindstromi*	*Cordylodus lindstromi*	490.0	0.709032
LR 137	451.1	Wilberns	U. Cambrian	*Cordylodus lindstromi*	*Cordylodus intermedius*	490.0	0.709025
TCU 78 (M)	450.3	Wilberns	U. Cambrian	*Cordylodus lindstromi*	*Teridontus nakamurai*	490.0	0.709084
TCU 75 (M)	449.4	Wilberns	U. Cambrian	*Clavohamulus hintzei*	*Teridontus nakamurai*	490.2	0.709008
TCU 73 (M)	446.8	Wilberns	U. Cambrian	*Clavohamulus hintzei*	*Teridontus nakamurai*	490.3	0.709019
LR 124	447.6	Wilberns	U. Cambrian	*Clavohamulus hintzei*	*Cordylodus* sp.	490.5	0.709029
TCU 65 (M)	446.4	Wilberns	U. Cambrian	*Hirsutodontus simplex*	*Teridontus nakamurai*	490.7	0.709023
LR 116	445.2	Wilberns	U. Cambrian	*Hirsutodontus simplex*	*Cordylodus proavus*	490.8	0.709039
TCU 56.5L (M)	443.8	Wilberns	U. Cambrian	*Hirsutodontus simplex*	*Teridontus nakamurai*	491.0	0.709041
TCU 56.0L (M)	443.6	Wilberns	U. Cambrian	*Clavohamulus elongatus*	*Teridontus nakamurai*	491.0	0.709021
TCU 55L (M)	443.3	Wilberns	U. Cambrian	*Clavohamulus elongatus*	*Cordylodus* sp.	491.0	0.709029
TCU 55L (M)	443.3	Wilberns	U. Cambrian	*Clavohamulus elongatus*	*Cordylodus* sp.	491.0	0.709021
LR 110	443.3	Wilberns	U. Cambrian	*Clavohamulus elongatus*	*Cordylodus proavus*	491.0	0.709031
TCU 52L (M)	442.4	Wilberns	U. Cambrian	*Clavohamulus elongatus*	*Cordylodus* sp.	491.0	0.709030
LR 105	441.5	Wilberns	U. Cambrian	*Clavohamulus elongatus*	*Cordylodus* sp.	491.1	0.709029
TCU 51 (M)	440.0	Wilberns	U. Cambrian	*Clavohamulus elongatus*	*Cordylodus* sp.	491.1	0.709036
TCU 51 (M)	440.0	Wilberns	U. Cambrian	*Clavohamulus elongatus*	*Eoconod. notchpeakensis*	491.1	0.709045
TCU 50.25 (M)	439.5	Wilberns	U. Cambrian	*Clavohamulus elongatus*	*Semiacontiodus nogamii*	491.1	0.709035
TCU 50.25 (M)	439.5	Wilberns	U. Cambrian	*Clavohamulus elongatus*	*Cordylodus* sp.	491.1	0.709042
LR 90	436.4	Wilberns	U. Cambrian	*Clavohamulus elongatus*	*Cordylodus intermedius*	491.2	0.709059
WR 34	434.2	Wilberns	U. Cambrian	*Clavohamulus elongatus*	*Cordylodus proavus*	491.3	0.709050
LR 80 (M)	433.3	Wilberns	U. Cambrian	*Clavohamulus elongatus*	*Cordylodus proavus*	491.3	0.709044
WR 26.25	430.8	Wilberns	U. Cambrian	*Fryxellodontus inornatus*	*Cordylodus proavus*	491.4	0.709040
WR 24.5	429.4	Wilberns	U. Cambrian	*Fryxellodontus inornatus*	*Cordylodus proavus*	491.4	0.709038

Table (Continued)

Lange Ranch, Welge Ranch, and Threadgill Creek, Llano uplift, Texas, USA (Cambrian-Ordovician transition)

Sample name	Height	Formation	System	Conodont biozone	Conodont material	Age (Ma)	^{87}Sr/^{86}Sr dyn.
LR 70 (M)	428.9	Wilberns	U. Cambrian	*Fryxellodontus inornatus*	*Cordylodus proavus*	491.4	0.709039
LR 64	426.8	Wilberns	U. Cambrian	*Hirsutododontus hirsutus*	*Cordylodus proavus*	491.5	0.709055
WR 18	425.6	Wilberns	U. Cambrian	*Hirsutodontus hirsutus*	*Cordylodus* sp.	491.5	0.709081
LR 55	423.5	Wilberns	U. Cambrian	*Cambrooistodus minutus*	*Eoconod. notchpeakensis*	491.6	0.709071
LR 45 (M)	420.5	Wilberns	U. Cambrian	*Cambrooistodus minutus*	*Cambrooistodus minutus*	491.6	0.709052

Oland, Sweden (Lower Ordovician: Tremadoc-"Arenig")

Sample name	Height	Formation	System	Fossil biozone	Conodont material	Age (Ma)	^{87}Sr/^{86}Sr dyn.
III/9	—	Kopingsklint	L. Ordovician	*Paroistodus evae*	*Drepanoistodus forceps*	475.0	0.708903
III/9	—	Kopingsklint	L. Ordovician	*Paroistodus evae*	*Drepanoistodus* sp.	475.0	0.708851
IV/IV	—	Djupvik	L. Ordovician	*Paroistodus evae*	*Drepanoistodus* sp.	475.0	0.708925
IV/IV	—	Djupvik	L. Ordovician	*Paroistodus evae*	*Drepanoistodus* sp.	475.0	0.708930
IV/II	—	Djupvik	L. Ordovician	*Drepanodus deltifer*	*Drepanoistodus* sp.	480.0	0.708865
II/3	—	Djupvik	L. Ordovician	*Drepanodus deltifer*	*Cordylodus* sp.	480.0	0.709060
III/1	—	Djupvik	L. Ordovician	*Cordylodus angulatus*	*Cordylodus angulatus*	489.5	0.709153

Djukte River, Siberia (Cambrian-Ordovician transition)

Sample name	Height	Formation	System	Fossil biozone	Conodont material	Age (Ma)	^{87}Sr/^{86}Sr dyn.
II-61	260.6	Urgorsian	L. Ordovician	Fauna D	*Drepanodus* sp.	483.8	0.708897
II-55	244.3	Urgorsian	L. Ordovician	Fauna D	*Drepanodus parallelus*	484.8	0.708732
II-52	241.8	Urgorsian	L. Ordovician	Fauna D	*Drepanodus* sp.	485.0	0.708939
II-42	238.5	Urgorsian	L. Ordovician	Fauna D	*Drepanodus* sp.	485.2	0.708727
II-36	231	Njajsian	L. Ordovician	Fauna C	*Drepanodus suberectus*	485.7	0.708922
II-27	228	Njajsian	L. Ordovician	Fauna C	*Scolopodus gracilis*	485.8	0.708963
II-24	227.6	Njajsian	L. Ordovician	Fauna C	*Drepanodus* sp.	485.9	0.708956
II-19	212	Njajsian	L. Ordovician	Fauna C	*Drepanodus* sp.	486.9	0.708986
II-4	195.8	Njajsian	L. Ordovician	Fauna C	*Cordylodus* sp.	487.9	0.708988
I-36	165.9	Loparian	U. Cambrian	*Cordylodus proavus*	*Cordylodus proavus*	491.5	0.708982
I-18	78.7	Loparian	U. Cambrian	*Cordylodus proavus*	*Cordylodus proavus*	491.5	0.709035
I-16	77.6	Mansian	U. Cambrian	*Eoconodontus*	*Eoconod. notchpeakensis*	492.3	0.708999
I-5-4	50.6	Mansian	U. Cambrian	*Eoconodontus*	*Eoconod. notchpeakensis*	492.3	0.709029
I-5-2	50.6	Mansian	U. Cambrian	*Eoconodontus*	*Eoconod. notchpeakensis*	492.3	0.708969

Khos-Nelege Section, Karaulakh Mountains, Kazakhstan (Lower-Upper Cambrian)

Sample name	Height	Formation	System	Fossil biozone	Brachiopod material	Age (Ma)	^{87}Sr/^{86}Sr dyn.
3-k	717	Ogon'or	?Ordovician	*Parabolinites levis*	inarticulate brachiopods	492	0.709218
k-17	674	Ogon'or	?Ordovician	*Parabolinites levis*	inarticulate brachiopods	493	0.709536
20-17-2	395	Ogon'or	U. Cambrian	*Glyptagnostus stolidotus*	inarticulate brachiopods	498	0.709385
20-14-9	377	Ogon'or	U. Cambrian	*Agnostus pisiformis*	inarticulate brachiopods	498	0.709383
20-5-1*	291	Ogon'or	M. Cambrian	*Anomocarioides limbataeformis*	inarticulate brachiopods	499	0.709418
y-89-5k	235	Mayaktakh	M. Cambrian	*Dorpyge olenekensis*	*Lingulata* sp.	503	0.709400
y-89-5a	182	Mayaktakh	M. Cambrian	*Comexochus tersus*	*Lingulata* sp.	507	0.709446
C-80/111-6e	178	Sekten	M. Cambrian	*Triplagnostus gibbus*	inarticulate brachiopods	508	0.709687
y-89-3e	167	Sekten	M. Cambrian	*Triplagnostus gibbus*	*Lingulata* sp.	508	0.709631
y-89-3g	165	Sekten	M. Cambrian	*Triplagnostus gibbus*	*Lingulata* sp.	509	0.709325
C-80/III-5	162	Sekten	M. Cambrian	*Kuonamcithes*	inarticulate brachiopods	509	0.709962
C-80/III-2	148	Sekten	L. Cambrian	*Bergeroniellus asiaticus*	inarticulate brachiopods	512	0.710095
C-80/II-9	125	Sekten	L. Cambrian	*Nelgeria lata*	inarticulate brachiopods	515	0.709416
C-80/1-3*	108	Tyuser	L. Cambrian	*Judomia*	inarticulate brachiopods	524	0.710046
C-80/1-2*	77	Tyuser	L. Cambrian	*Judomia*	inarticulate brachiopods	528	0.709707
2/8*	51	Tyuser	L. Cambrian	*Nevadella*	inarticulate brachiopods	529	0.710030
2/6*	32.7	Tyuser	L. Cambrian	*Aldanocyathus sunnaginicus*	inarticulate brachiopods	530	0.709468
2/2*	28.1	Tyuser	L. Cambrian	*Aldanocyathus sunnaginicus*	inarticulate brachiopods	530	0.709967

Obulus Sandstone, Estonia (Middle Cambrian-Lower Ordovician)

Sample name		Formation	System	Stratigraphic level/biozone	Brachiopod material	Age (Ma)	^{87}Sr/^{86}Sr dyn.
L-10/4	—	Tosna	?Ordovician	*Rhabdin. norvegica. (Cord. ang.)*	*Obulus apollinis*	?>489	0.709161
E-29/2	—	basal Tosna	?Ordovician	? base *Cordylodus angulatus*	*Helmersenia ladogensis*	?>489	0.709145
L-1/3 (0.8–1.9)	—	Tosna	U. Cambrian	? *Cordylodus lindstromi*	*Obulus apollinis*	?>489	0.708862

(Continued)

Table (Continued)

Obulus Sandstone, Estonia (Middle Cambrian-Lower Ordovician)

Sample name		Formation	System	Stratigraphic level/biozone	Brachiopod material	Age (Ma)	^{87}Sr/^{86}Sr dyn.
E-22a-3	—	Maardu mb.	U. Cambrian	*Cordylodus andresi*	*Schmidtites cellatus*	?>491	0.709139
L-10/6	—	Tosna	?U. Cambrian	(redeposited)	*Schmidtites cellatus*	?>491	0.709121
190/36.6–36.9	—	Lomashka	U. Cambrian	*Cordylodus andresi*	*Schmidtites cellatus*	?>491	0.709142
L-31/1	—	Tosna	?U. Cambrian	(redeposited)	*Schmidtites cellatus*	?>491	0.709142
190/36.9–37.3	—	Lomashka	U. Cambrian	*Cordylodus andresi*	*Schmidtites cellatus*	?>491	0.709087
L-2/3	—	Ladoga	?U. Cambrian	(? redeposited)	*Ungula convexa*	Up. Cam.	0.708861
K-20/6	—	Tosna	?U. Cambrian	(redeposited)	*Obulus apollinis*	Up. Cam.	0.709126
K-20/6	—	Tosna	?U. Cambrian	(redeposited)	*Schmidtites cellatus*	Up. Cam.	0.709120
L-1/13	—	Ladoga	?U. Cambrian	(? *in situ*)	*Rebrovia* sp.	Up. Cam.	0.708896
L-1/13	—	Ladoga	?U. Cambrian	(redeposited)	*Ungula cf. convexa*	Up. Cam.	0.708884
E-26/4	—	Ulgase	U. Cambrian	l-lower part III	*Rebrovia chernetskae*	Up. Cam.	0.709111
E-4/6	—	Ulgase	U. Cambrian	l-lower part III	*Oepikites fragilis*	Up. Cam.	0.709102
L-17/7	—	basal Ladoga	U. Cambrian	I-II	*Ungula* sp.	Up. Cam.	0.708895
L-47/8	—	basal Tosna	?U. Cambrian	(redeposited)	*Ungula* sp.	Up. Cam.	0.709109
L-19/3	—	upper Sablinka	M.Cambrian	*?Paradoxides forchhammeri*	*Oepikites kolchanovi*	Mid. Cam.	0.709111

Alum Shale, Sweden (Middle Cambrian)

Sample name	Height	Formation	System	Fossil biozone	Paraconodont material	Age (Ma)	^{87}Sr/^{86}Sr dyn.
6172	—	Alum Shale	M. Cambrian	Vb	*Hertz. elongata*	499	0.716152
5659	—	Alum Shale	M. Cambrian	Vc	*Furn. ovata*	498	0.710385
6747	—	Alum Shale	M. Cambrian	II	*Hertz. elongata*	501	0.713289
6404	—	Alum Shale	M. Cambrian	II	*Furn. mullerina*	501	0.712776
6404	—	Alum Shale	M. Cambrian	II	*West.* sp.	502	0.712455
6760	—	Alum Shale	M. Cambrian	I	*Hertz. elongata*	502	0.710901
6414	—	Alum Shale	M. Cambrian	I	*Furn.* sp.	502	0.711931
6414	—	Alum Shale	M. Cambrian	I	*West. quadrata*	502	0.712368
6730	—	Alum Shale	M. Cambrian	I	*West.* sp.	502	0.712211

Dayangcha Section, Xiaoyangqiao, Jilin Province, China (Cambrian-Ordovician transition)

Sample name	Height	Section	System	Conodont biozone	Sample material	Age (Ma)	^{87}Sr/^{86}Sr dyn.
HDA 31-5	144	XCS	L. Ordovician	*Cordylodus angulatus*	*Teridontus* sp.	489.5	0.709026
HDA 15A	101.2	XCS	L. Ordovician	*lapetognathus jilinensis*	inarticulate brachiopods	489.9	0.709927
HDA 14-2	100.4	XCS	L. Ordovician	*lapetognathus jilinensis*	inarticulate brachiopods	489.9	0.709903
HDA 14-2	100.4	XCS	L. Ordovician	*lapetognathus jilinensis*	*Cordylodus* sp.	489.9	0.7.09234
HDA 11A-3	96.9	XCS	U. Cambrian	*Cordylodus intermedius*	*Teridontus* sp.	491.0	0.709178
22.0–22.3	90.4	XCS	U. Cambrian	*Upper Cordylodus proavus*	*Cordylodus* sp.	491.2	0.709255
21.62–22.0	90.1	XCS	U. Cambrian	*Upper Cordylodus proavus*	*Cordylodus* sp.	491.2	0.709228
21.45–21.62	89.8	XCS	U. Cambrian	*Upper Cordylodus proavus*	*Cordylodus* sp.	491.2	0.709152
21.17–21.34	89.5	XCS	U. Cambrian	*Upper Cordylodus proavus*	*Cordylodus* sp.	491.2	0.709189
20.59–20.7	89	XCS	U. Cambrian	*Upper Cordylodus proavus*	*Cordylodus* sp.	491.2	0.709260
20.91–20.17	88.9	XCS	U. Cambrian	*Upper Cordylodusproavus*	*Cordylodus* sp.	491.2	0.709270
HDA 9B-2	88.9	XCS	U. Cambrian	*Upper Cordylodus proavus*	inarticulate brachiopods	491.2	0.710091
HDA 9B-2	88.9	XCS	U. Cambrian	*Upper Cordylodus proavus*	*Prooneotodus rotundatus*	491.2	0.709347
20.45	88.8	XCS	U. Cambrian	*Upper Cordylodus proavus*	*Cordylodus* sp.	491.2	0.709382
19.85–20.1	88.4	XCS	U. Cambrian	*Upper Cordylodus proavus*	*Cordylodus* sp.	491.2	0.709207
19.5–19.6	88	XCS	U. Cambrian	*Upper Cordylodus proavus*	*Cordylodus* sp.	491.2	0.709199
HDA 9A-1	87.8	XCS	U. Cambrian	*Upper Cordylodus proavus*	*Prooneotodus rotundatus*	491.2	0.709340
HDA 9A-1	87.8	XCS	U. Cambrian	*Upper Cordylodus proavus*	inarticulate brachiopods	491.2	0.709550
19.25	87.7	XCS	U. Cambrian	*Upper Cordylodus proavus*	*Cordylodus* sp.	491.2	0.709234
18.7–18.95	87.3	XCS	U. Cambrian	*Middle Cordylodus proavus*	*Cordylodus* sp.	491.5	0.709182
18.28–18.47	86.8	XCS	U. Cambrian	*Middle Cordylodus proavus*	*Cordylodus* sp.	491.5	0.709168
18.1	86.5	XCS	U. Cambrian	*Middle Cordylodus proavus*	"Acanthodus shergoldi"	491.5	0.709051
17.2	85.1	XCS	U. Cambrian	*Middle Cordylodus proavus*	*Cordylodus* sp.	491.5	0.709196
17	84.9	XCS	U. Cambrian	*Middle Cordylodus proavus*	*Cordylodus* sp.	491.5	0.709330
HDA 9-9	84.7	XCS	U. Cambrian	*Middle Cordylodus proavus*	*Prooneotodus rotundatus*	491.5	0.709225
16.7	84.6	XCS	U. Cambrian	*Middle Cordylodus proavus*	*Cordylodus* sp.	491.5	0.709200
13.2–13.25	82.2	XCS	U. Cambrian	*Lower Cordylodus proavus*	*Cordylodus* sp.	491.5	0.709290
HDA 7-3	80.7	XCS	U. Cambrian	*Lower Cordylodus proavus*	*Prooneotodus rotundatus*	491.5	0.709479
HDA 7B-1	80.3	XCS	U. Cambrian	*Lower Cordylodus proavus*	*Prooneotodus rotundatus*	491.5	0.710187
9.2–9.3	77.6	XCS	U. Cambrian	*Lower Cordylodus proavus*	*Cordylodus* sp.	491.5	0.709175
HDA 2-D	72.6	XCS	U. Cambrian	*Cambrooistodus*	*Phakelodus tenuis*	491.7	0.709669
JD 11-1	53.3	XLS	U. Cambrian	*Proconodontus mulleri*	*Prooneotodus rotundatus*	492.7	0.709337

(Continued)

Table (Continued)

Dayangcha Section, Xiaoyangqiao, Jilin Province, China (Cambrian-Ordovician transition)

Sample name	Height	Section	System	Conodont biozone	Sample material	Age (Ma)	$^{87}Sr/^{86}Sr$ dyn.
JD 9-6	41.3	XLS	U. Cambrian	*Proconodontus posterocostatus*	*Phakelodus tenuis*	493.0	0.710218
JD 7-1	18.5	XLS	U. Cambrian	*Proconodontus posterocostatus*	*Phakelodus tenuis*	493.0	0.709865
JD 6-1	14.7	XLS	U. Cambrian	*Proconodontus posterocostatus*	*Prooneotodus rotundatus*	493.0	0.709970
JD 6-1	14.7	XLS	U. Cambrian	*Proconodontus posterocostatus*	inarticulate brachiopods	493.0	0.709886
JD 4-3	8.9	XLS	U. Cambrian	*Proconodontus tenuiserratus*	*Prooneotodus rotundatus*	493.2	0.709811